THE REPUBLIC OF TURKEY
BAHCESEHIR UNIVERSITY

MOLECULAR MECHANISM OF AT1R/PARP1 INHIBITORS INTERACTIONS USING COMBINED MOLECULAR MODELING APPROACHES AND PHYSICS-DRIVEN VIRTUAL IDENTIFICATION OF NOVEL THERAPEUTICS AGAINST RETINAL INFLAMMATION

MASTER'S THESIS

MD KAMRUL HASAN

ISTANBUL, 2021

THE REPUBLIC OF TURKEY
BAHCESEHIR UNIVERSITY

GRADUATE SCHOOL
BIOENGINEERING MSc (THESIS)

MOLECULAR MECHANISM OF AT1R/PARP1 INHIBITORS INTERACTIONS USING COMBINED MOLECULAR MODELING APPROACHES AND PHYSICS-DRIVEN VIRTUAL IDENTIFICATION OF NOVEL THERAPEUTICS AGAINST RETINAL INFLAMMATION

MASTER'S THESIS

MD KAMRUL HASAN

Thesis Supervisor: PROF. DR. SERDAR DURDAĞI

ISTANBUL, 2021

T.C.

BAHCESEHIR UNIVERSITY

GRADUATE SCHOOL

...../...../.....

MASTER THESIS APPROVAL FORM

This thesis has been approved by the Graduate School which has fulfilled the necessary conditions as Master thesis.

Program Name:	Master's in Bioengineering
Student's Name and Surname:	Md Kamrul Hasan
Name Of The Thesis:	Molecular Mechanism of AT1R/PARP1 Inhibitors Interactions Using Combined Molecular Modeling Approaches And Physics-driven Virtual Identification Of Novel Therapeutics Against Retinal Inflammation.
Thesis Defense Date:	25/06/2021

Assoc. Prof. Dr. Burak KÜNTAY

Institute Director

This thesis was read by us, quality and content as a Master's thesis has been seen and accepted as sufficient.

	Title/Name	**Signature**
Thesis Advisor's	Prof. Dr. Serdar Durdağı	
Member's	Assist. Prof. Dr. Timuçin Avşar	
Member's	Assoc. Prof. Dr. Mert Gür	

DECLARATION

I hereby declare that this project is my own work and that to the best of my knowledge and belief, it contains no material previously published or written by another person nor material which has been accepted for the award of any other degree except where due acknowledgment has been made in the text.

Date: _____

Signature: _____

(Md Kamrul Hasan)

ACKNOWLEDGEMENT

I want to express my deepest appreciation to my thesis advisor Prof. Dr. Serdar Durdağı. He conveyed a spirit of excitement towards research, scholarship, and teaching in a consistent and loveable way. Without his excellent and huge experienced guidance and continuous support and help, this thesis wouldn't have been possible.

I would like to thank all Durdagi Lab members for their help, support, and friendly environment. The person without whom it would be almost impossible to learn new things is Ismail Erol. He was always there for any kind of difficult situation. Busecan Aksoydan was also an exceptionally supportive person, who was always there to answer any problems or questions in lab work.

It would be hard without supportive and friendly lab members, and I would like to thank Lalehan Oktay, Asena Himmetoğlu, and Gurbet Tutumlu for their support and helpful nature.

I am also very grateful to my family. Without their contribution and support, it would be impossible to study in a foreign country. My father, Md Shahidullah, supported me all the way he could do for my education. Especially I would like to thank my sister Farzana Afrin, my brother-in-law Tauhidur Rahman, and my brother Mohibul Hasan, who have always encouraged me towards my way.

Without everyone's positive support, I would never be able to come this far.

Istanbul, 2021 Md Kamrul Hasan

ABSTRACT

MOLECULAR MECHANISM OF AT1R/PARP1 INHIBITORS INTERACTIONS USING COMBINED MOLECULAR MODELING APPROACHES AND PHYSICS-DRIVEN VIRTUAL IDENTIFICATION OF NOVEL THERAPEUTICS AGAINST RETINAL INFLAMMATION

Md Kamrul Hasan

Bioengineering MSc (Thesis)

Thesis supervisor: Prof. Dr. Serdar DURDAĞI

June 2021, 96 pages

The classic renin-angiotensin system (RAS) is known as a homeostasis regulator of blood pressure and electrolyte. It has recently been recognized as a pro-inflammatory mediator and implicated in various age-related ocular disorders associated with the activation of inflammatory molecules. The findings of RAS components in the eye initiate a new therapeutic approach to alleviate ocular disorders through RAS inhibitors such as angiotensin-II type-I receptor (AT1R) antagonists. It is shown that retinal microglia express AT1R, and their activation state is significantly altered by its endogenous ligand Ang-II. Thus, Ang-II may directly activate the AT1Rs on microglia and contribute to retinal inflammation, such as in diabetic retinopathy, an increase in Ang-II levels play an important role. AT1R is a class A G protein-coupled receptor (GPCR). GPCRs may exist and function as monomers; however, they can assemble to form higher-order structures, and as a result of oligomerization, their function and signaling profiles can be altered. Recent findings reveal that AT1R can form homodimers and activate the non-canonical (β-arrestin-mediated) pathway. Since it is shown that microglia-mediated inflammation response in the retina has been associated with the development of retinal degenerations and because of therapeutic effects of PARP1 inhibitors on retinal degeneration, in this study, known PARP1 inhibitors have interacted with the AT1R and molecular mechanism studies have been carried out using integrated molecular modeling approaches including molecular docking, molecular dynamics (MD) simulations, post-processing MD analyses.

Keywords: Molecular docking, Molecular Dynamics simulations, Ocular Disorders, Angiotensin II Type I Receptor.

ÖZET

Kombine Moleküler Modelleme ve Fizik-temelli Sanal Tarama Yaklaşımları ile AT1R/PARP1 İnhibitörlerinin Retinal İnflamasyona Karşı Yeni Terapötikler Olarak Belirlenmesi ve Moleküler Mekanizmalarının Araştırılması

Md Kamrul Hasan
Biyomühendislik
Tez danışmanı: Prof. Dr. Serdar DURDAĞI
Haziran 2021, 96 sayfa

Klasik renin-anjiyotensin sistemi (RAS) elektrolit ve kan basıncının homeostaziz regülatörü olarak bilinmektedir. Son zamanlarda bir pro-inflamatuar aracı olarak kabul edilmiştir ve inflamatuar moleküllerin aktivasyonu ile ilişkili yaşa bağlı çeşitli oküler bozukluklarda rol oynadığı anlaşılmıştır. Gözdeki RAS bileşenlerinin bulguları, anjiyotensin-II tip-I reseptör (AT1R) antagonistleri gibi RAS inhibitörleri aracılığıyla oküler bozuklukları hafifletmek için yeni bir terapötik yaklaşım başlatmaktadır. Retinal mikroglianın AT1R'ü eksprese ettiği ve aktivasyon durumlarının endojen ligandı Ang-II tarafından önemli ölçüde değiştirildiği gösterilmiştir. Bu nedenle, Ang-II, mikroglia üzerindeki AT1R'leri doğrudan aktive edebilmekte ve diyabetik retinopatide olduğu gibi retina inflamasyonuna katkıda bulunabilmektedir, dolayısıyla Ang-II seviyelerindeki artışın hastalıkta önemli bir rol oynadığı anlaşılmıştır. AT1R, bir sınıf A G protein-bağlı reseptördür (GPCR). GPCR'lar monomer olarak bulunabilmekte ve işlev görebilmektedir; bunun yanında daha yüksek mertebeden yapılar oluşturmak üzere bir araya gelebilmekte ve oligomerizasyon sonucunda işlevleri ve sinyal oluşurma profilleri değiştirilebilmektedir. Son bulgular, AT1R'nin homodimerler oluşturabileceğini ve kanonik olmayan (β-arrestin aracılı) yolu aktive edebileceğini ortaya koymaktadır. Retinada mikroglia aracılı inflamasyon yanıtının retina dejenerasyonlarının gelişimi ile ilişkili olduğu ve PARP1 inhibitörlerinin retina dejenerasyonu üzerindeki terapötik etkileri nedeniyle bu çalışmada, bilinen PARP1 inhibitörlerinin AT1R'e bağlanmaları hesaplamalı yöntemlerle test edilmiştir. Bu çalışmada, moleküler kenetleme, Moleküler Dinamik (MD) simülasyonlar, ve MD sonrası analizler dahil olmak üzere entegre moleküler modelleme yaklaşımları kullanılarak hit moleküller belirlenmiş ve moleküler mekanizma çalışmaları gerçekleştirilmiştir.
Anahtar Kelimeler: Moleküler kenetleme, Moleküler Dinamik simülasyonlar, Oküler Bozukluklar, Anjiyotensin II Tip I Reseptör.

TABLE OF CONTENTS

TABLES

FIGURES

ABBREVIATIONS

2D	:	Two dimensional
3D	:	Three dimensional
ACE	:	Angiotensin Converting Enzyme
ACEI	:	Angiotensin-Converting Enzyme Inhibitors
AGTR1	:	Angiotensin II Receptor Type I Gene
ALA	:	Alanine
Ang I	:	Angiotensin I
Ang II	:	Angiotensin II
ARB	:	AT1 Blocker
ARG	:	Arginine
ASN	:	Asparagine
ASP	:	Aspartic Acid
AT1R	:	Angiotensin II Receptor Type I
AT2R	:	Angiotensin II Receptor Type II
BP	:	Blood Pressure
C Terminal	:	Carboxy-Terminal
CADD	:	Computer-aided drug design
CCR5	:	C-C Chemokine Receptor Type 5
Cryo-EM	:	Cryoelectron Microscope
CYS	:	Cysteine
D3	:	Dopamine 3
D3R	:	Dopamine 3 Receptor
DPPC	:	Dipalmiyol Phosphatidyl Choline
EC	:	Extracellular
ECL	:	Extracellular Loop
EMEA	:	European Medicines Agency
FDA	:	Food and Drug Administration
GBSA	:	Generalized Born Solvent Accessible Surface Area
GDP	:	Guanosine diphosphate

GLN	:	Glutamine
GLU	:	Glutamic Acid
GLY	:	Glycine
GPCR	:	G Protein-Coupled Receptors
GROMACS	:	Groningen Machine for Chemical Simulations
GTP	:	Guanosine Triphosphate
H-bond	:	Hydrogen Bond
HIS	:	Histidine
HTVS	:	High Throughput Virtual Screening
IC	:	Intracellular
ICL	:	Intracellular Loop
ICM	:	Internal Coordinate Mechanics
IFD	:	Induced Fit Docking
ILE	:	Isoleucine
L	:	Ligand
LBDD	:	Ligand Based Drug Design
LEU	:	Leucine
LINCs	:	Linear Constraint Solver
LQTS	:	Long QT Syndrome
LYS	:	Lysine
MD	:	Molecular Dynamics
MET	:	Methionine
N – Terminal	:	Amino Terminal
NMR	:	Nuclear Magnetic Resonance
NOP	:	Nociceptine/Orphanian FQ Peptide Receptor
OPLS	:	Optimized Potential for Liquid Simulations
OPM	:	Orientation in Protein Membranes
PBC	:	Periodic Boundary Conditions
PDB	:	Protein Data Bank
PARP	:	Poly ADP Ribose Polymerase
PHE	:	Phenyl alanine
PME	:	Particle mesh Evald

POPC	:	Palmitoyl Oleyol Phosphatidyl-Choline
PRO	:	Proline
QM	:	Quantum Mechanics
QPLD	:	Quantum-Polarized Ligand Docking
QSAR	:	Quantitative Structure-Activity Relationship
RAS	:	Renin Angiotensin System
RMSF	:	Root Mean Square Fluctuation
SBDD	:	Structure-Based Drug Design
SD	:	Steepest Descent
SER	:	Serine
SP	:	Standard Precision
THR	:	Threonine
TM	:	Transmembrane
TRP	:	Tryptophan

1. INTRODUCTION

Retinopathy is a trait that results from the complication of diabetes, as well as a leading cause of blindness in working-age people (Sjølie & Chaturvedi, 2002). The angiotensin II type-1 receptor (AT1R) gene is an important target for preventing retinopathy development (Rübsam et al., 2018). Sufficient evidence proves that the angiotensin system is adequately expressed in the eye, and AT1R blockers can function in the inhibition of angiogenesis (Kurihara et al., 2012). PARP1 (Poly Adenosine Di-Phosphate-Ribose Polymerase) is a protein, involved in the renin-angiotensin system (RAS) related disease (Reinemund et al., 2009).

The RAS or renin-angiotensin-aldosterone system (RAAS) is a hormone system, responsible for regulating blood pressure, fluid and electrolyte balance and vascular resistance. Angiotensinogen, released from the liver, is converted to angiotensin I. Angiotensin-converting enzyme (ACE) converts angiotensin I to angiotensin II (Ang-II). Increased blood pressure generally occurs, due to the narrowing of blood vessels by potent vasoconstrictive peptide, Ang-II. Ang-II is responsible for activating the Ang-II type I receptor (AT1R) and Ang-II type II receptor (AT2R). Suppression and overstimulation of these receptors can result in hypertension, renal failure, coronary artery, and diabetic retinopathy. AT1R blockers (ARBs) or ACE inhibitors (ACEIs) are the currently used therapeutics for this complex health problem.

The “sartan” family consists of a newer group of pharmaceuticals, like losartan, candesartan, valsartan, irbesartan, telmisartan, eprosartan, azilsartan and so on. They all act on AT1R, and work as an antagonist. For RAAS pathway, AT1R antagonist works very specifically and selectively on AT1R target, while in Ang-II synthesis pathway, they work independently. As a result, blockade of AT1R mediated effects of Ang-II have become more selective in comparison with ACE inhibitors.

AT1Rs are known as members of the class A G Protein Coupled Receptor (GPCR) family, which is a membrane protein family with a significant role in signal transduction. They have seven trans-membrane (TM) domains, associated with intracellular and extracellular loops (ICL, ECL) (De Gaspero et al., 2000). According to recent reports, AT1R blockers

can function as potential anticancer agents, by suppressing cell growth, stimulated by Ang-II (Kawai et al., 2017). It has been reported that retinal microglia express AT1R, and Ang-II can alter their activity. As a result, Ang-II can directly act on AT1R activity on microglia and contribute to retinal inflammation. Recent studies revealed that AT1R monomers can form homodimers, resulting in the activation of the non-canonical (β-arrestin mediated) pathway (Jean-Charles et al. 2017). In the regulation of adaptive immune response, the effector molecules in RAS, specifically, Ang-II and its AT1R, where Ang-II was proposed to contribute in pro-inflammatory effects. (Kunert-Radek et al. 1994). Moreover, it is not clear enough how AT1R plays role in antigen specific T (a type of lymphocyte) cells. In T cell activation, the proliferation, adhesion and differentiation are triggered by Ang-II, which acts like as co-stimulatory molecule (Coppo et al. 2017). In the higher production of pro-inflammatory cytokines by CD+ T cells, AT1R is actively involved, which results in added capacity, to stick with and migrate by contributing on up regulation of chemokine receptors (Silva-Filho et al., 2016).

PARP1 is an essential protein for repairing DNA in cancer cells. Uncontrolled PARP1 activity may cause stroke, myocardial infarction, neurodegeneration and some other disease conditions. PARP1 inhibitors conduct to trapping of PARP proteins on DNA to inhibit their catalytic action, that stands in the way of replicating DNA and resulting in the death of cancerous cells (Patel et al. 2020). Recent studies have shown that PARP1 inhibitors have therapeutic effects on retinal degeneration. The first approved PARP1 inhibitor was Olaparib (Lynparza™), which was used for BRCA1 or BRCA mutation treatment for women in Europe (Tomao et al. 2020). PARP is a broad family, consisting of 18 proteins, where nicotinamide adenine dinucleotide (NAD+) are utilized as substrate (Amé et al., 2004). It has two subtypes of PARP1 and PARP2, which are activated by damaged DNA and triggers repairing of DNA pathways (Y. Q. Wang et al., 2016). When it binds to damaged DNA, the catalytic activity of PARP1 is increased. Other proteins, in DNA damaged sites are added by this auto poly ADP ribosylation and as a result, it creates a repairing complex. (Sun et al., 2018)

In the beginning stage of drug discovery, primary task starts by identifying a lead compound. The structural optimizations of the lead compound for a better therapeutic

activity and potency is the next step. In drug discovery process, high-throughput screening (HTS) is widely used, which is mainly designed for producing quantitative data on the activity of thousands of chemicals, towards hundreds of biological targets and pathways. Nowadays, HTS is being largely used for screening large compound libraries for identification of lead compounds, which has been popular in pharmaceutical industries. But, the drawback of HTS is, it's very expensive process and at the same time, finding active compound with their actual mechanism cannot be assured. As a result, adapting structure-based drug design, using computational approaches, are highly increased in the phase of finding a lead compound. Computer-aided drug design has become a high-priority tool in the drug discovery and development approaches, in recent years. A drug may be a substance that binds to a specific target macromolecule receptor, to exert pharmacological effects. Drug discovery is the foremost field in analysis; however, the method is time-consuming, and costs a lot, for searching a new hit compound (Lionta et al., 2014). It has been published that for an era, too many docking programs have been developed with a rewarding success in virtual screening application procedure. But the drawback is, few programs show false negative (compounds that are active, but not representing top ranking scores in docking softwares) and false positives (compounds showing highest scores in ranking, but, are inactive). For specific receptor or class of compounds, some individual docking programs, most of the time, show impressive capability in case of predicting higher affinity compounds. In order to be successful in docking application, appropriate target structure with experimental knowledge, is the top priority throughout the procedure.

At present time, in understanding molecular mechanism processes, structure-based drug design (SBDD) acts by using the structure of protein for discovering new ligands or small molecule (Ferreira et al. 2015). SBDD is playing focused role for efficiently developing therapeutic agents. Since SBDD targets for disease in molecular level and uses three-dimensional structural knowledge of the biological target or protein, it has been proven much more efficient than other tools of drug discovery. It is possible now to get experimental results in atomic level, as investigation of molecular interaction of ligand-protein binding can be done. For delivering new drug molecules in a very quicker and cost-effective way, computational tools now play a very advantageous role in drug

discovery process. Alternative approaches of HTS are SBDD, including virtual screening (VS) and de novo drug design, which have proved much more efficient in drug molecule searching procedure. Commercially available drug molecules or drug-like compounds can be screened using computational tools, towards target or protein of known structure, in large drug compound libraries and at the same time, some compounds, that are predicted to bind well, can be tested experimentally (Sliwoski et al., 2014). In the SBDD process, 3D target structural information of interest, is the primary thing to begin with. It can be obtained from experimental data, like X-ray crystallography, nuclear magnetic resonance (NMR) or homology modeling techniques can be used to model the 3D structure of the target protein.

The aim of this thesis study, to repurpose PARP1 inhibitors on AT1 receptor. Since recent findings proved that both PARP1 and AT1R play an important role in retinopathy, already available PARP1 inhibitors can be used to block AT1R. Successful candidates can act on both PARP1 and AT1R, and may provide better therapeutic activity to cure retinopathy.

1.1 Theoretical Background

1.1.1 Computer-aided Drug Design (CADD) Approaches

Drug discovery and development is a prolonged and complex process, in which computer aided drug design (CADD) has become the one of the most significant approaches in present era. (Figure 1.1) A drug can be defined as a ligand, when it binds to a specific biological target or protein to execute necessary therapeutic effects. The drug discovery process is very expensive process. It is known that it may costs $800 million up to the US $2 billion from the scientific reports, and at the same time, it may takes 10-15 years for the approval, production and marketing of the drug product from drug searching is started (Paul et al. 2010).

Figure 1.1: The representative workflow of CADD.

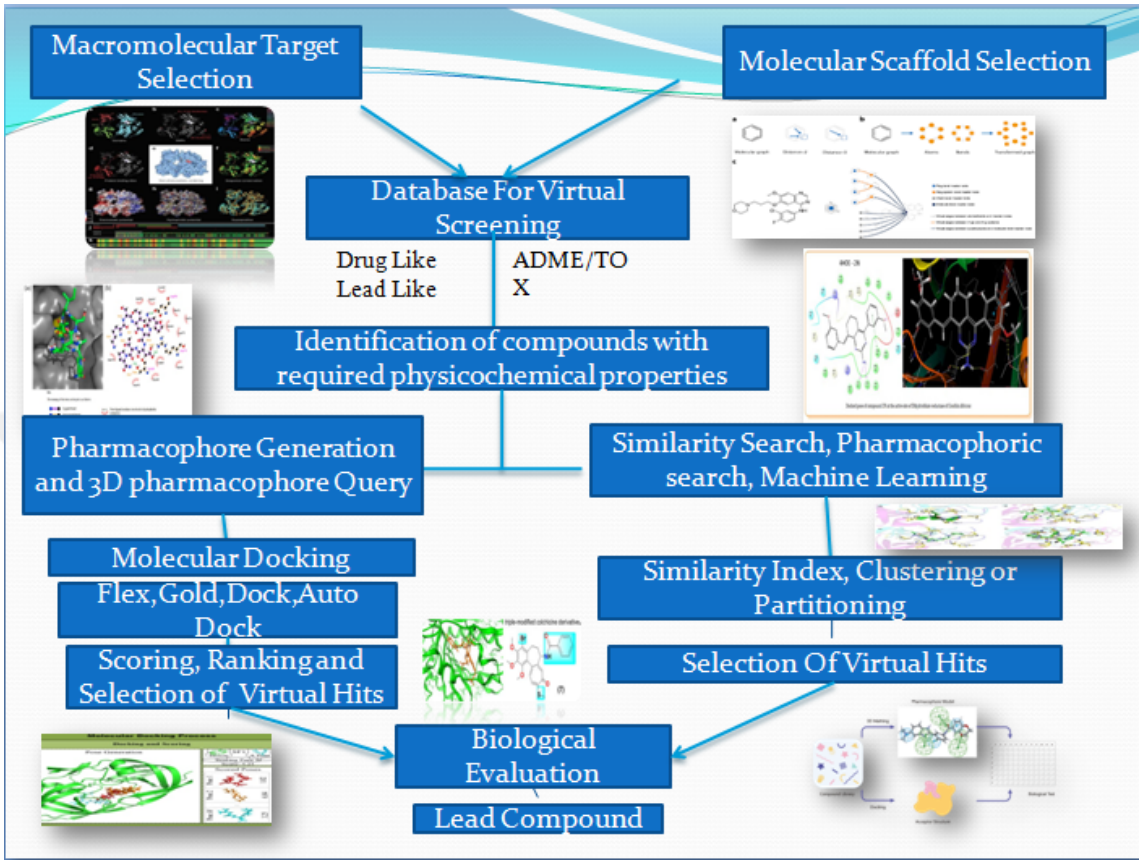

(Source: Adapted from (Talevi, 2018))

CADD plays a vital role in discovering the drug molecule process for screening enormous compound libraries, into the compact collection of functional compounds. CADD fundamentally, relies on ligand-based drug design (LBDD), and SBDD. SBDD requires target protein structure information, to calculate the binding energies of all studied compounds (Yu & Mackerell. 2017). When there is no 3D structural information of the target protein or if the homology modeling studies may not be applied, LBDD techniques such as quantitative structure activity relationships (QSAR) models can be constructed to represent a pseudo binding pocket of the target protein. The impact of structural factors on biological activity can be investigated using QSAR modeling.

In the process of structure-based virtual screening (SBVS) an important step is the construction of the compound database. There are drug like molecules in SBVS database,

which are available freely. Lipinski's rule of five (Bialystok, 2017) ensures drug likeliness of a compound, stating that the molecular weight of an ideal drug like compound should be lower than 500 Da, logP (lipophilicity) value should be lower than 5, hydrogen bond donor number less than 5, and hydrogen bond acceptors less than 10. Metabolically liable moieties, and known toxic compounds must be excluded, along with lead like properties screening.

SBDD, mostly, begins by screening a possible substance with a binding affinity, precisely, to the target molecule. The substance binding sites, are referred to as the active sites. Structure-based approaches mostly depend on three dimensional (3D) structures of target information. (Lionta et al., 2014) Active compounds, against specific targets are searched mainly at the active site. Target structures are retrieved at the molecular level, using X-ray diffraction (XRD), solution and solid state nuclear magnetic resonance (NMR), electron microscopy, neutron diffraction, electron crystallography, solution scattering, and fiber and powder diffraction methods. Macromolecule databank (protein data bank, PDB, rcsb.org) (Berman et al., 2002) currently contains more than 180.000 available structures among them more than 88% are solved using X-ray crystallography. Without the target macromolecule structure's atomic positions, the 3D structure, can be modeled and predicted with homology modeling. In homology modeling, a solved target structure from same family can be used as template structure.

Molecular docking is an approach, for predicting the bioactive conformation of compounds in target structures, calculates interactions between protein and ligand molecules. (Figure 1.2) In which, ligand conformation in a binding pocket, and accurate prediction of the binding energy plays a vital role. To be fitted into the binding pockets of proteins, ligand searches for various conformations. The electrostatic, van der Waals interactions, hydrogen bonding, inhibitor strain, enzyme desolvation, are important factors for free energy calculation of the protein-ligand complex (Kitchen et al. 2004)

Figure 1.2: Bioactive conformation and binding energy of a ligand can be predicted with molecular docking approach.

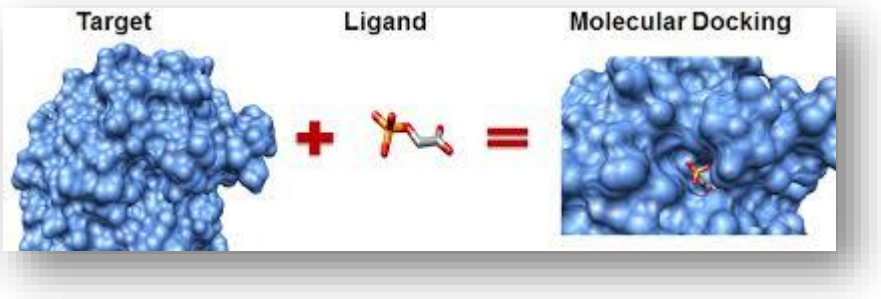

(Source: Adapted from (Yang et al., 2020))

$$\Delta G = RTlnK_d = \frac{[L][P]}{[LP]} \quad \text{.....(1.1)}$$

In Equation 1.1, calculation of binding free energy of the ligand at the target protein (ΔG) from dissociation constant (K_d) is represented. The binding of the ligand to the target protein will be tighter, if the value of ΔG becomes the lowest. In molecular docking, ΔG can be predicted with the summation of binding interaction forces between ligand and target protein atoms. (Equation 1.2) Calculation of docking algorithm, via ΔG can provide information about binding free energy of ligand, although, recent docking algorithms provide only static information. Degrees of freedom become very large, when, both flexible parts of ligand and protein are taken, requiring costly computer sources. As a result, flexibility is given only in docked ligand at the binding pocket, and the target site, where, minimal flexibility is taken. Flexibility of the ligand and binding pocket residues can be increased with Induced Fit Docking (IFD) protocols. (Eunsung Mouradian, 2008)

$$\Delta G_{bind} = \Delta G_0 + \Delta G_{h-bonds} \sum_{h-bonds} f(\Delta r, \Delta\alpha) + \Delta G_{arom} \sum_{arom} f(\Delta r, \Delta\alpha) + \Delta G_{ionic} \sum_{ionic} f(\Delta r, \Delta\alpha) + \Delta G_{lipo} \sum_{lipo} |A_{lipo}| + \Delta G_{rot}\, N_{rot} \quad \text{.....(1.2)}$$

In Equation 1.2, ΔG_0 , refers to, standard binding free energy. $\Delta G_{h-bonds}$ describes the contribution of hydrogen bonds to the binding free energy. ΔG_{ionic} refers the contribution from an unperturbed ionic interactions. ΔG_{arom} describes the contribution of the binding free energy of aromatic interactions. ΔG_{lipo} describes the contribution of binding free energy from lipophilic interactions. ΔG_{Rot} describes rotational penalties, that are applied to the binding free energies.

Docking is a static approach. In order to better understand that structural and dynamical profiles of the interactions between protein-ligand complexes, molecular dynamics (MD) simulations can be performed. MD simulations play an important role in protein motion determining, thus plays significant role in drug discovery (Salo-ahen et al., 2021). NMR, X-ray crystallography and homology modeling help in building a static model, which can provide important insights for macromolecular structure determination. In case of a drug or small molecule binds to a receptor, it does not interact with a single, frozen structure, it interacts with a macromolecule in a constant motion, but, if the protein motion are limited, then the ligand can fit into static binding pocket like a key fits into lock (A & VA, 2018). The idea of MD simulation is, calculating the force applied on each atom by all rest of other atoms with the help of using Newton's law of motion, for getting a prediction of the spatial position of each atom, as a function of time. Specifically, calculating the forces on each atom continuously, and after that updating the position and velocity of each atom by using these forces, which results in trajectory, describing configuration of the system at every point throughout the simulation time at atomic level. These simulations capture the position and motion of every atom in every point of time. By comparing simulations, the variety of molecular perturbations can be analysed (Scott A. Hollingsworth & Ron O. Dror, 2018).

In LBDD approach, QSAR method is the widely used technique which uses known experimental knowledge, to develop a general pharmacophore model (Verma et al., 2010). Molecules with similar structures, tend to own similar biological activity. Validation, of the overall pharmacophore model can be done using alternative ligands with known experimental activity. Combination of these approaches can create a chance to find new drug molecules. The most considerable distinction between ligand-based and

structure-based approaches is the 3D structural information of the target protein data. Data, on receptor spatial coordinates, and their active sites are not required in QSAR. To derive data from ligands, initially, their experimental activities ought to be known. There need to be enough ligands with a diverse biological of activities (i.e., from micromolar to nanomolar).

1.1.2 GPCR Signaling Pathway

RAS is the endocrine system, that controls plasma blood pressure (Preston et al., 1998). Proteinase in circulation, transforms vasoconstrictor to hypertensin (Ang I), and primarily, cleaves ten residues of angiotensinogen. These cleaved residues tagged Ang I, in which, decapeptide (Arg-Val-Tyr-Ile-His-Pro-Phe-His-Leu) is remodelled into hypertensin octapeptide (Ang II) by ACE, in the main respiratory organ capillaries. ACE cleaves peptide linkage between Phe and Ang I, C-terminal residues and Ang-II induces vessel narrowing, along with, targeting AT1R. Often, Ang-II induces mineralocorticoid endocrine secretion, which mediates urinary organ metallic element (Na^+) organic process, and potassium (K^+), which implicitly affects body pressure level. Excessive RAS stimulation induces several diseases and high blood pressure; diseases like, arteria coronaria, viscus attack, obesity, diabetic kidney disease, urinary organ disorder, and cancer, which are also regulated through ACEIs, ARBs, proteinase inhibitors that specifically, block Ang II. Targeted medications are usually used as strategies of medical aid. Another Ang-II target is AT2 receptor. Its functional roles have not been fully clarified yet (Sallander et al. 2016, Durdagi et al. 2018).

GPCRs are one of the cell membrane macromolecules of superfamilies, that process chemical secretion messengers and release neurotransmitters (D. Wang, 2018; Fredriksson et al. 2003a). GPCRs incorporate seven alpha-helical trans-membrane (TM) domains, connected by three extracellular (EC) and three intracellular (IC) loops, headed by EC amino-terminal (N-terminal) and IC carbon-terminal (Zhou et al., 2019). These categories include category A (rhodopsin-like), category B (secretin receptor family), category C (metabotropic glutamate), category D (pheromone plant receptor), and category F -frizzled (FZD) and smoothened (SMO) receptors. Categories D and E for invertebrates. GRAFS is an alternate vertebrate theme. Vertebrate GPCRs have five

completely different families; Glutamate, Rhodopsin, Adhesion, Secretin and Frizzled/Taste2 (Fredriksson et al., 2003b). Binding of ligand molecule to target GPCR causes conformational change of the protein. This alteration affects GPCR-G macromolecule interaction, and remodelling of downstream proteins (O'Connor, 2010; Inoue et al. 1997), (Figure 1.3). The increased understandings of GPCR structure have made a parallel increase in GPCR targeting drug designing studies (Cherezov et al., 2007, Kruse et al., 2012).

Figure 1.3: GPCR signaling pathway.

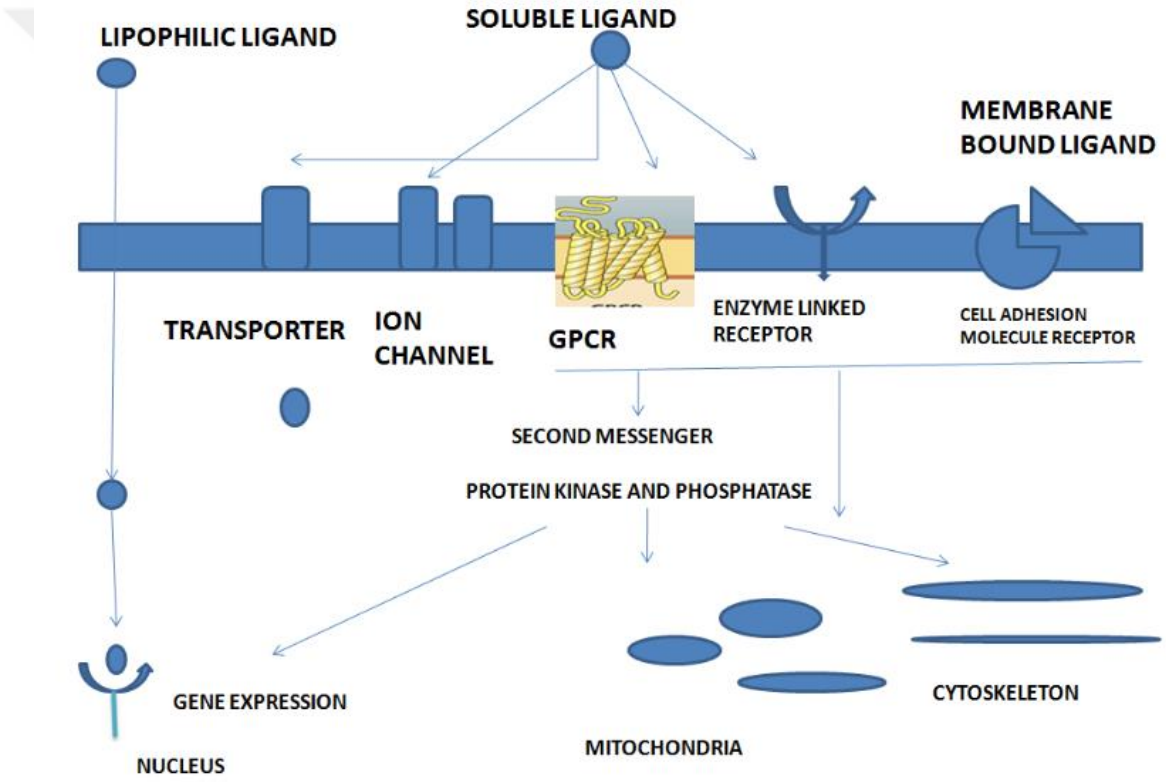

(*Source: Adapted from (Gurevich & Gurevich, 2019)*)

AT1R plays a significant role in regulation of cardiovascular and renal homeostasis, though, overstimulation of AT1R can cause hypertension and hypertrophy like diseases. AT1R blockers are now widely used for these types of diseases. AT1R ligand may also activate the beta-arrestin mediated pathway. (Figure 1.4)

Figure 1.4: Beta-arrestin mediated pathway.

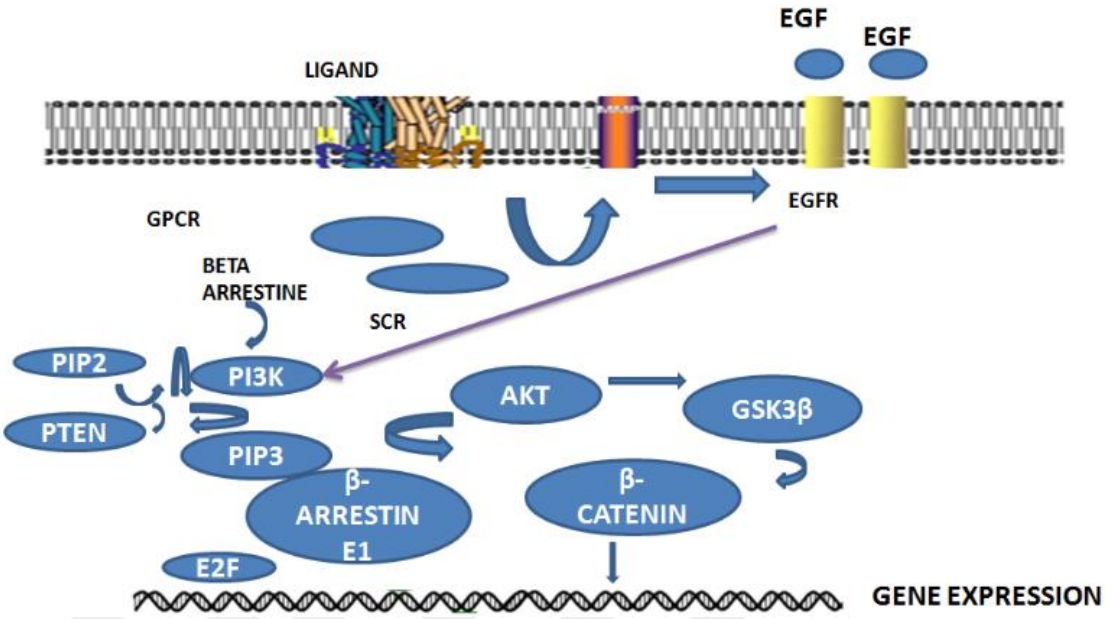

(Source: Adapted from (Van Gastel et al., 2018))

1.1.3 Diabetic Retinopathy

Persons with diabetes, eventually, suffer from microangiopathy of retina, called diabetic retinopathy, which can be subdivided into two types; like, diabetic macular edema and proliferative retinopathy. Among them, macular edema can highly threaten visual impairment. Arterial blood pressure, plays a significant role in development and progression of diabetic retinopathy, which has become the leading cause of blindness among working age people (Ulbig & Kollias, 2010). Figure 1.5 shows diabetic retinopathy pathway.

Figure 1.5: Diabetic retinopathy pathway.

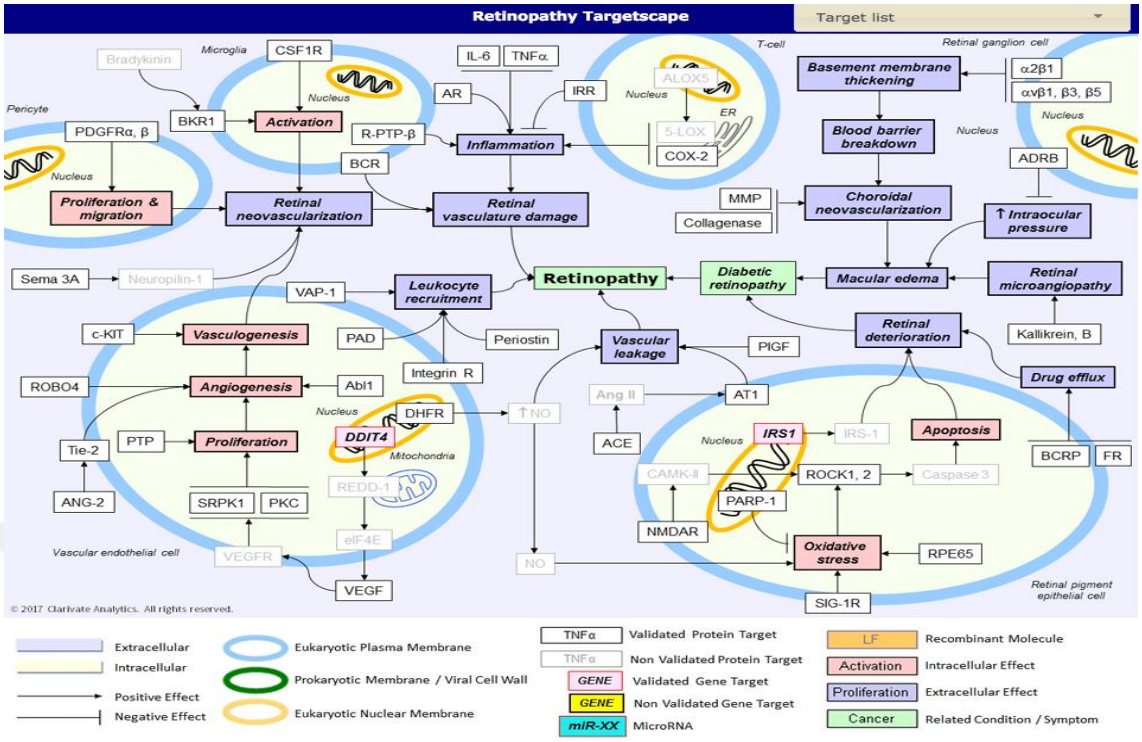

1.1.4 PARP1

PARP1 is a protein, involved in DNA repair, which is activated by DNA strand breaks (Ko & Ren, 2012; Murata et al., 2019; Chen, 2011). PARP1 is composed of three functional domains (Figure 1.5). PARP1 needs two zinc fingers, which can be found on amino-terminal DNA-binding domain for binding with single-strand breaks and double strand –breaks. (Huambachano et al., 2011).

Figure 1.6: Structural along with functional organization of PARP1.

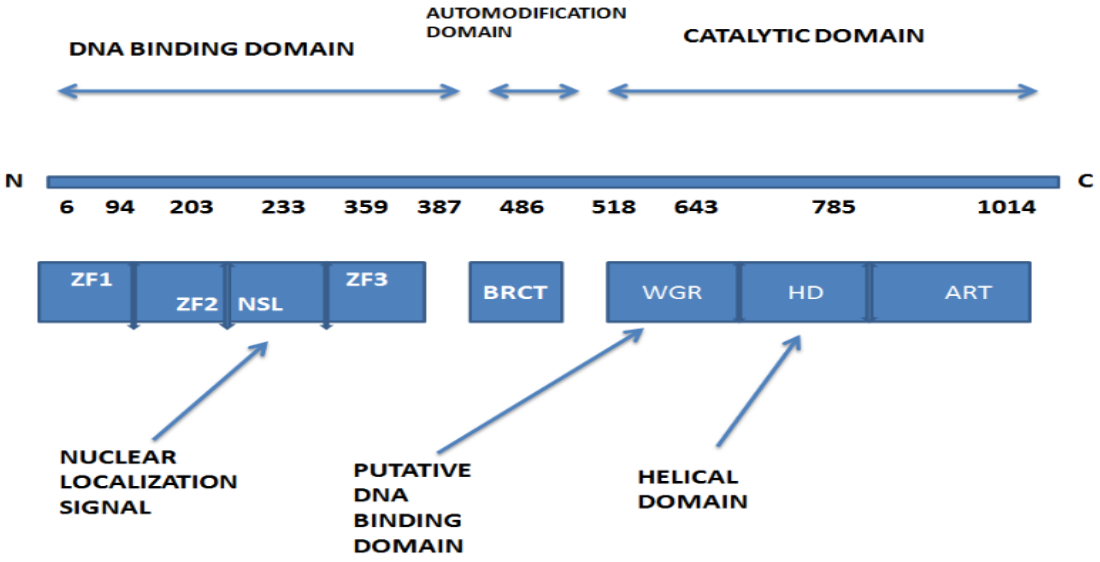

(Source: Adapted from (Eustermann et al. 2015)).

1.1.5 Aim of the Study

In this study, molecular docking, MD simulations, molecular mechanics generalized Born surface area (MM/GBSA) binding free energy calculations were performed, to analyse the AT1/PARP1 interactions, and their molecular mechanisms. In this thesis, computational approaches, like, molecular docking, MD simulations and post-processing MD analyses were combined to determine inhibitors of PARP1 interactions with AT1R. The highlights would represent the molecular mechanism, that would be useful for further designing of potent inhibitors, to cure diabetic retinopathy.

2. LITERATURE REVIEW

In 1995, Feng *et al*. stated about a direct charge pair by applying bold interaction in between Ang-II and Arg2 side chain along with Asp281 of the receptor which led to partial agonism. It happened as arginine side chain was being able to take part in different hydrogen bonding interactions (Feng et al. 1995)

In 2001, Nikiforovich &Marshall studied structure activities with various analogues of Ang-II , which showed the importance of Arg2, Tyr4, His6 and Phe8 and also the importance of negatively charged carboxy terminal regions for Ang-II (Nikiforovich & Marshall 2001).

In 2002, Gradman discussed in their paper about the pharmacological properties and clinical efficacy of the AT1R blockers, which differed markedly. Without affecting maximal response, losartan shifted the dose-response curve for Ang-II to the right. By increasing the concentration of Ang-II, losartan could act as unsurmountable antagonist.

In 2015, Haitao *et al.* used crystal structure human AT1R in complex with Olmesartan (Benicar TM), which is an inverse agonist and highly potent antihypertensive drug for the regulation of blood pressure, for identification of specific interactions between AT1R and different ARBs. It was observed in the study that binding of endogenous peptide agonist is affected by the mutation N1113.35A in the putative binding site (Haitao et al., 2015).
In 2011 Miura *et al.* stated in their paper about highly selective ARBs. The main focus of the study was the class effects versus molecular effects (Miura et al., 2011).

In 2013, Akazawa *et al.* published a work that demonstrated that Ang-II through AT1Rs was able to stimulate multiple signaling pathways and transfers with various tyrosine kinases along with increased rate of transcription of growth factor receptors (Akazawa et al., 2013).

In 2013, Miura *et al.* published their work about the molecular mechanisms of non-peptide AT1 receptor antagonists act different as variations of their molecular structures (Miura et al. 2013).

In 2013, Fillion *et al.* stated that in their paper about binding of the Ang-II at different sites of the receptors in the extracellular loops (ECL) along with transmembrane helices. They mentioned that the bound Ang-II was adopting vertical binding mode along with it's amino terminus and it's carboxy terminus was interacting more strongly in between the transmembrane domain core (Fillion et al. 2013).

In 2016, Silva-Filho *et al.* discussed in their paper about the axis of RAS, AngII and its receptor, AT1R, played role as an important effector by regulating T-cell responses. By using tools of pharmacology, these studies characterized effects of AngII, and AT1R. The specific function did AT1R play, in antigen specific CD8+ T cells, was not known. This study revealed that in antigen specific CD8+ T cells and AT1R regulated expansion, differentiation and function during effector and memory phase during response against plasmodium (Silva-Filho et al., 2016).

In 2020, Anderson *et al.* stated in their paper about AT1R blockers, which are the commonly prescribe drugs, in treatment of cardiovascular disease. Due to non-synonymous single nucleotide polymorphisms, (nsSNPs) within the AT1R gene, the effectiveness of ARBs varies largely. There were 100 nsSNPs, which could be found in AT1R coding sequence. However, for the determination of nsSNP, which nsSNP could abrogate the binding with selective ARBs, was the purpose of this study. (Anderson et al., 2020).

In 2015, Malyuchenko *et al.* stated in their paper about the discovery of antitumor drugs, targeting the PARP1. In some disease, associated with neoplasm and lung cancer, breast cancer expression of PARP1 was observed. By aiming at DNA binding and transcriptional activity, rather than aiming catalytic domain could open the possibility of developing new PARP1 inhibitors, which was discussed in this paper (Malyuchenko et al., 2015).

In 2020, Zhang et al discussed in their paper about PARP1 inhibitors, which were derived from various pyridopyridazione derivatives. The isostere of pthalazine nucleus of the lead compound Olaparib, using pyridopyridazinone scaffold, was used, to modify the tail part of the molecule. Most compounds possessed inhibitory potencies in nanomolar level in

comparison with Olaparib. As a reference, drug with 8a (IC_{50}=36nM), with compared to Olaparib, showed, best PARP1 inhibitory action. The newly designed compound was docked well into PARP1 active site, and at the same time, their complexes were stabilized by three key hydrogen bond interactions with both Gly863, Ser904, along with favourable π-π and hydrogen-π stacking interactions with Tyr907 and Tyr896, which was revealed by molecular modeling (Zhang et al., 2020).

3. COMPUTATIONAL METHODS

3.1 Protein Preparation

A reasonable beginning structures of ligand and protein, is the prerequisite for desired campaigning of SBVS. There are heavy atoms present in an ideal PDB structure file (in case of X-ray structure), and at the same time, water molecules, co-factors, ligands, metal ions, along with various protein subunits are also present in a typical PDB structure. But, about bond orders, formal atomic charges or topologies, there is limited information in the structure. Low resolution of a specific protein area, may result in missing of larger loops or residue side chains. There are some protein preparations schemes that have been proposed to resolve above mentioned structural issues. (Lorenz-Fonfria, 2020) The proposed strategy starting from determining the protonation states of the amino acid residues. Some few popular softwares are PROPKA (Breiding, 2014), H++ (Davies et al., 2006). Later step, begins with assigning hydrogen atoms and protein hydrogen bond optimization, in accordance with, an ideal hydrogen bond network. The next step starts with assigning of partial charges, capping of residues, filling up missing side chains and loops, treating metals, and for relieving steric clashes the protein structure is minimized. A decision should be made whether, which water molecules will be removed or kept at the binding pocket, which can be done by WaterMap (Bolcato et al., 2020), JAWS (Trist et al., 2008), 3D RISM (Nguyen et al., 2019) in commercially available softwares.

In this study, the crystal structure of the AT1R (PDB ID: 4YAY) (Zhang et al., 2015b) were used. Protein preparation tool of Maestro molecular modelling package was used to prepare the AT1R structure. (Sastry et al., 2013) Before optimization and minimization, the mediator residues, from Asp1002 to Leu 1106, in the AT1R crystal structure, were removed, as, it was used to get the crystal structure with cytochrome. Hydrogen atoms were added, bond orders were allocated, disulphide bonds were generated between Cys18 and Cys274 and between Cys101 and Cys180. Missing side chains and loops were fixed. Prime module of the Maestro was used for the refinement of the target protein. Structural optimization were conducted at physiological pH 7.4, by running PROPKA (Bas et al.,.2008, Li et al., 2005). As force field OPLS3e was used for energy minimization.

3.2 Ligand Preparation

ChEMBL (https://www.ebi.ac.uk/chembl/) is considered as bioactivity database, where data extraction from medicinal chemistry literature and new sources of bioactivity data can be found. In the current study, 2499 PARP1 inhibitors and 1156 ATR1 binders and 20 AT1R approved drugs and ligands in clinical investigation were downloaded. For the preparation of the structures of ligand, LigPrep module was used. The OPLS3e force field was performed for structural optimization of the ligands. Protonation circumstances of ligands were allocated with running EPIK, and pH was adjusted to neutral 7.0 (Greenwood et al., 2010, Shelly et al., 2007) and generate all combinations were assigned. After completion, 4461 PARP1 inhibitors were generated. Settings were the same for preparation of the 1156 AT1R binding molecules and 20 AT1R drugs, which resulted into 2034 and 54 molecules, respectively.

3.3 Molecular Docking

Currently there freely available and commercial molecular docking programs such as Autodock, Glide, FlexX, GOLD, LigandFit (Z. Wang et al., 2016). Docking programs can be used to predict the binding poses of the ligands at the target structure as well as differentiate the strong binders from weak binders. (Huang & Zou, 2010) Glide/SP (standard precision) module of the Maestro molecular modeling package was used for molecular docking. (Friesner et al., 2004a, Friesner et al., 2006, Halgren et al., 2004). A grid map was built at the known active site of the AT1R crystal structure (Zhang et al., 2015b). The prepared grid AT1 crystal structure is indicated in Figure 3.1. Default settings of Glide were used in docking calculations.

Figure 3.1: Grid map of AT1R prepared for docking studies.

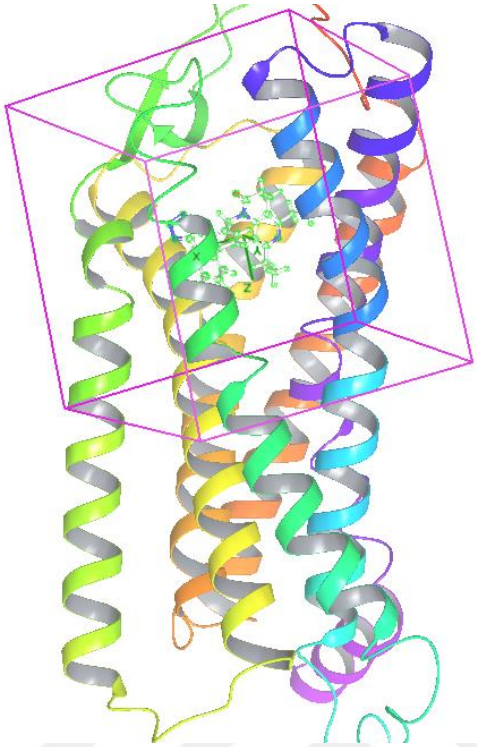

In the rotatable group's tab, all bonds as rotatable were assigned. Glide/SP docking protocol of Maestro molecular modeling package was used to dock 4461 PARP1 inhibitors at the AT1R. At the same time, 2034 AT1R binding molecules and 54 AT1R inhibitors were docked to the AT1R binding pocket.

3.3.1 Induced Fit Docking (IFD)

Induced fit docking protocol (IFD) along with Glide/Extra precision (XP) protocol of Maestro molecular modeling package was used for the selected compounds. At the beginning, for every ligand, Glide docking was performed. Selections of the ligands along with sample ring conformations were done and trimming of side chains were performed. Refinement of residues were set within 5 Å of ligand poses and optimization of side chains were done. This resulted in formation of a ligand structure and conformation, which acted as induced fit for every pose of the structure of the receptor. Ultimately, Glide re-docking was run in default settings and for precision, XP was selected. In the induced fit receptor structure, the ligand was precisely docked.

3.4 Molecular Dynamics (MD) Simulations

MD simulations were performed under physiological conditions for the analyses of structural and dynamic profile of the ligand-protein interactions. The protein-ligand input structures, used for MD simulations, were determined, in accordance with, the top-scored complex from IFD docking protocol. The MD simulations were carried out using Desmond (Ivanova et al., 2018) program. Simulations were carried out with the body temperature (310 K) and a pressure of 1 bar was applied in three runs along with *NPT* ensemble. Time step was 2 fs and the simulation length was 100 ns for each run. The OPLS3e force field parameters were used in all simulations (Roos et al., 2019). As it is membrane protein, POPC was used as lipid bilayer, OPM server was used for the alignment with crystal structure. The long-range electrostatic interactions were calculated using the particle mesh Ewald method. The Martyna–Tuckerman–Klein chain coupling scheme with a coupling constant of 2.0 ps was used for the pressure control and the Nosé–Hoover chain coupling scheme for the temperature control. The trajectories were saved at 50 ps intervals for analysis.

3.5 Molecular Mechanics Generalized Born Surface Area (MM/GBSA) Calculations

MM/GBSA method was run to estimate ligand-binding affinities, using molecular mechanics and continuum solvent models (Rastelli et al., 2010). For protein-ligand binding free energy calculations, the Prime-MMGBSA module was used. Solvation model VSGB 2.0 and force field OPLS3e was used for calculation.

3.6 Binary QSAR Models

MetaCore /Metadrug is a web-based platform, where it uses developed binary QSAR models, for predicting therapeutic activity, and at the same time, toxicity and pharmacokinetic profile prediction of screening molecules (Durdagi et al., 2020).

The structures of top 20-PARP1 identified inhibitors were submitted to MetaCore/ MetaDrug, for the purpose of analysing therapeutic activity. MetaDrug uses Tanimato prioritization (TP) for finding the similarity between analysed compound and compounds in the construction of QSAR models, based on the elements that can be found in structures. In this application, the predicted values are normalized between 0 and 1, where 0 refers to inactive and 1 refers to active molecules.

4. RESULTS

4.1. Molecular Docking Studies

2499 PARP1 inhibitors were collected from ChEMBL database. These molecules were prepared before the docking calculations, after the ligand preparation because of different protonation states and stereochemistries, total number of compounds reached to 4461. Before the docking, capability of the used docking software (Glide) to capture the correct co-crystallized pose of the ligand was evaluated. For this aim, co-crystallized ligand (ZD7) at the AT1R was removed from binding pocket and re-docked. RMSD between co-crystallized pose and docking pose were found as 0.7 Å both in Glide/SP and Glide/IFD methods. (Table 4.1) Since for Glide/SP and IFD, root mean square deviation (RMSD) values are below 1 Å, predicted pose of PARP1 inhibitors at the binding pocket of AT1R can be used confidently.

Table 4.1: Comparison of co-crystallized ligand (ZD7) conformation and top-docking pose.

	GLIDE/SP -Standard Precision	IFD-(Induced Fit Docking)
RMSD (Å)	0.70	0.70

Figure 4.1 represents distribution of docking scores of PARP1 inhibitors at the AT1R binding site. Most of the docked molecules have docking scores between -6 and -7 kcal/mol. Table 4.2 represents selected top-docking scored compounds.

Figure 4.1: Distribution of docking scores of PARP1 inhibitors at the AT1R binding site.

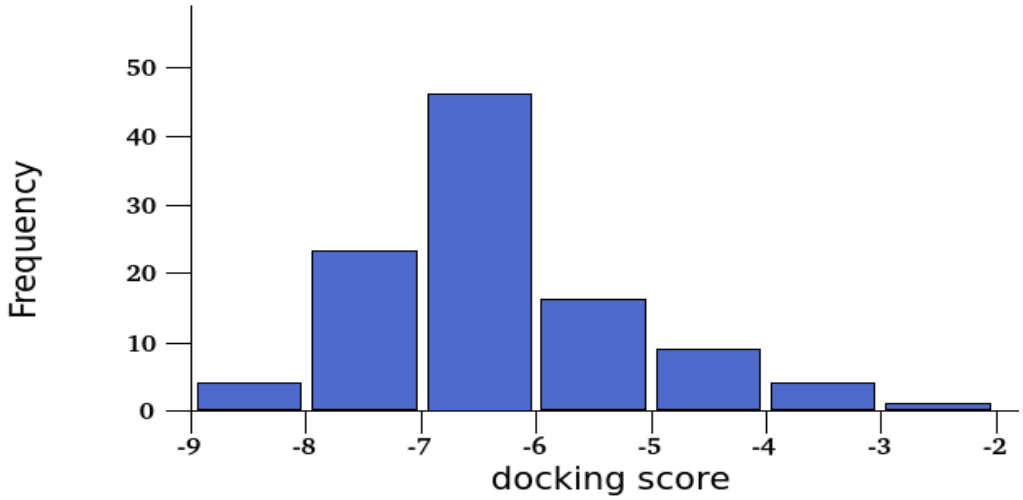

Table 4.2: Top-scored Docking, along with MM/GBSA free energy estimation result of PARP1 inhibitors, against the binding pocket of AT1R (Docking scores are in kcal/mol)

PARP1 INHIBITORS	**2D STRUCTURES**	**SP DOCKING kcal/mol**	**IFD DOCKING kcal/mol**	**MM/GBSA BIND kcal/mol**
CHEMBL 523887	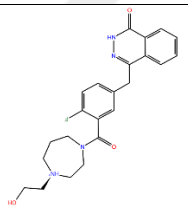	-10.01	-8.86	-83.92
CHEMBL 3945618	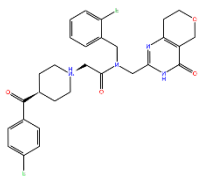	-9.73	-10.16	-64.27
CHEMBL 3317902	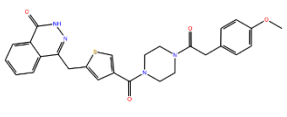	-9.00	-10.45	-89.51

CHEMBL 610491	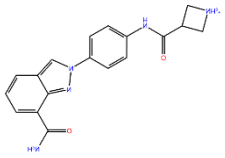	-8.80	-8.76	-63.17
CHEMBL 593609	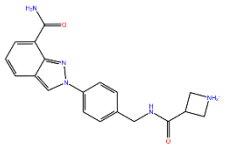	-9.15	-9.97	-56.83
CHEMBL 378794	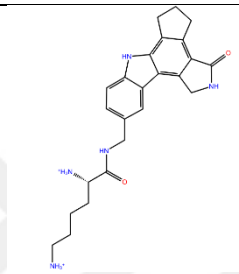	-8.94	-8.30	-41.30
CHEMBL 3933577	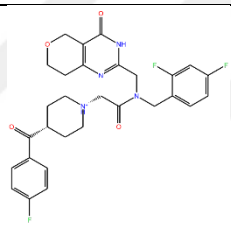	-8.79	-9.21	-61.54
CHEMBL 3105882	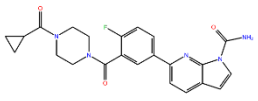	-8.98	-10.79	-68.05
CHEMBL 2323533	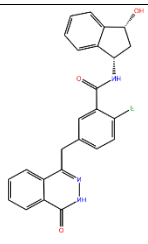	-8.79	-9.25	-82.10

CHEMBL 4177163	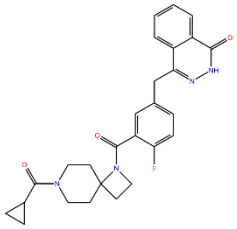	-8.84	-9.81	-72.46
CHEMBL 610165	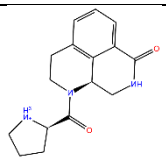	-9.25	-8.17	-50.83
CHEMBL 3663637	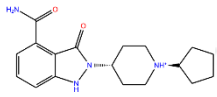	-9.00	-10.67	-65.25
CHEMBL 407760	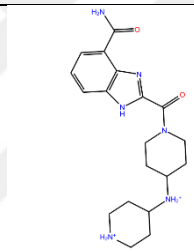	-8.98	-8.44	-58.60
CHEMBL 4084234	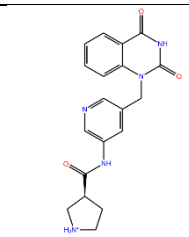	-8.78	-9.60	-60.20
CHEMBL 4167820	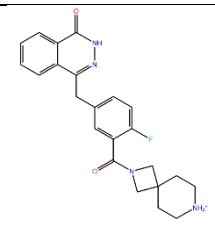	-8.82	-8.64	-69.53
CHEMBL 3649746	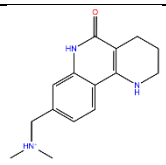	-8.80	-7.26	-42.13

CHEMBL 3922251	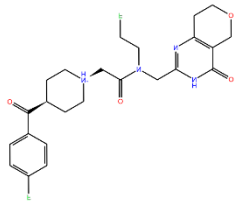	-9.03	-9.20	-58.41
CHEMBL 3891789	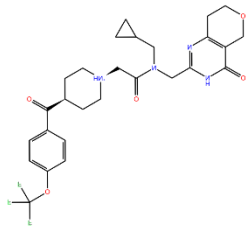	-8.83	-11.37	-61.03
CHEMBL 3644592	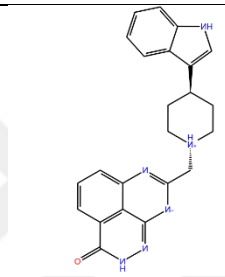	-8.90	-8.84	-36.46

Compound CHEMBL3891789 was found to top IFD docking score (-11.37 kcal/mol). Its corresponding Glide/SP docking scores was calculated as -8.83 kcal/mol. 2D and 3D ligand-residue interactions of this compound was depicted at Figure 4.2.

Figure 4.2: 2D and 3D ligand interaction diagrams of CHEMBL3891789 at the binding pocket of the AT1R.

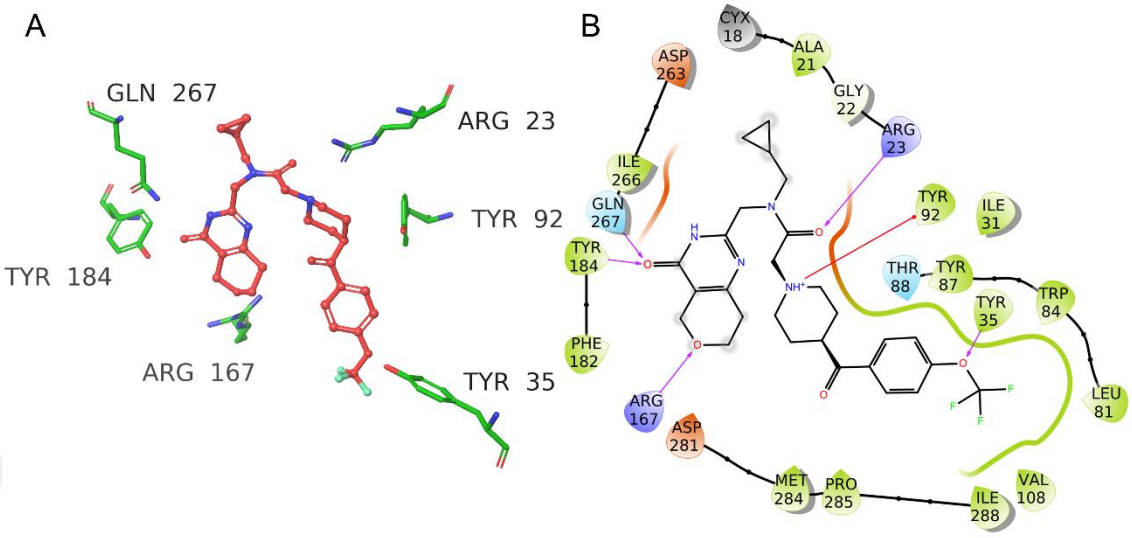

Figure 4.2 shows that while the residue Tyr92 is forming cation-pi interactions, Arg23, Tyr35, Arg167, Tyr184, and Gln267 form hydrogen-bonding interactions with the ligand. These residues are well-known residues for the crucial interactions of the known ARBs. Table 4.3 summarizes the crucial residues and their corresponding type of interactions with the binding pocket residues for the selected top-3 compounds.

Table 4.3: Top-scored compounds with their docking scores along with their residue interactions at the active site of the ATR1.

Selected PARP1 Inhibitors	**Docking Score (IFD)** **(kcal/mol)**	**Type of interactions**	**Amino Acid Residues at the Active Site**
CHEMBL3891789	-11.37	Hydrophobic, Hydrogen bond (backbone), Hydrogen bond (side chain)	Tyr92, Arg167, Gln267, Tyr184, Tyr35.
CHEMBL3105882	-10.79	bond(backbone), Hydrogen bond (side chain	Tyr92, Asp281, and Trp84.

CHEMBL3663637	-10.67	Hydrophobic, Hydrogen bond(backbone), Hydrogen bond (side chain	Tyr92, Asp281, and Trp84

1156 ATR1 binders and 20 AT1R approved drugs and ligands in clinical investigation were downloaded from ChEMBL after ligand preparation, total number of compounds were 2034 and 54 molecules, respectively. Figures 4.3 and 4.4 represent docking score distribution of the docked compounds.

Figure 4.3: Docking score distribution of the AT1R drugs and candidates.

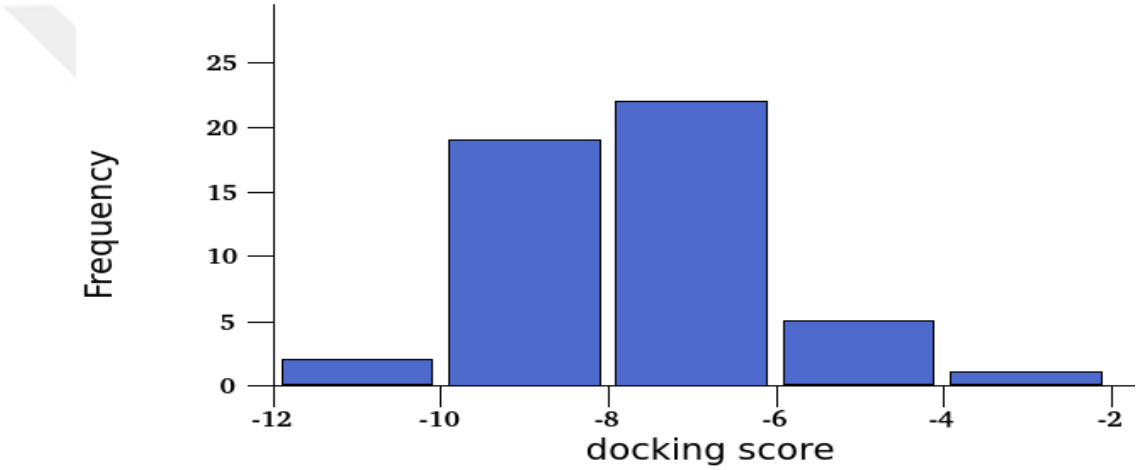

Figure 4.4: Docking score distribution of the AT1R binders.

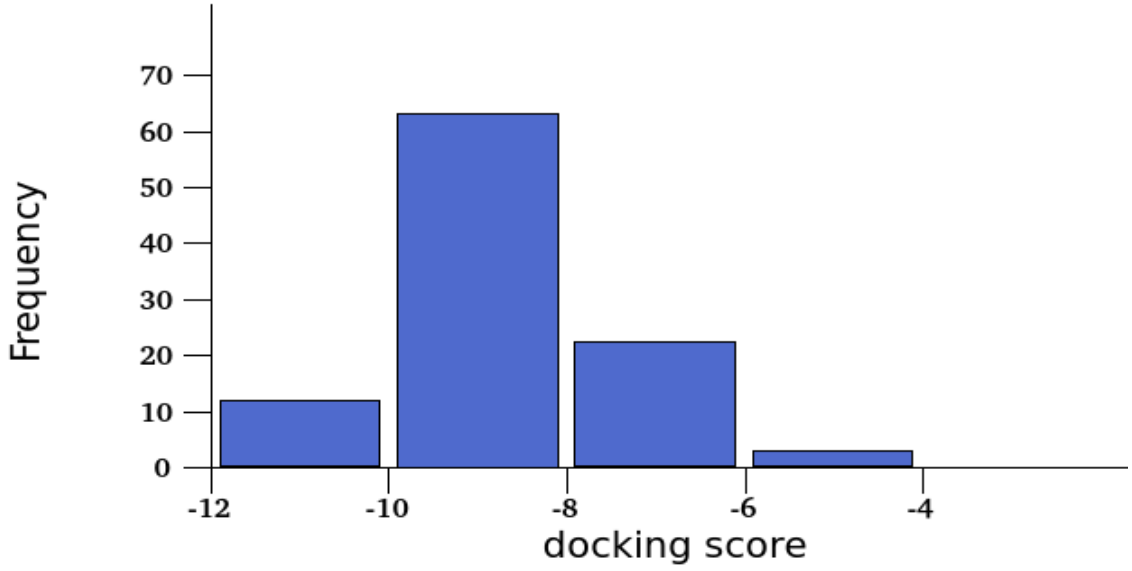

Table 4.4 represents the 2D structures and docking scores of selected ATR1 drugs and drugs in clinical investigation at the active site of the target protein.

Table 4.4: Top scored docking score and MMGBSA energy calculation of AT1 drugs and candidates at the binding pocket of AT1 (docking scores are in kcal/mol).

AT1 Drugs and Candidates	**GLIDE/ IFD (kcal/mol)**	**GLIDE/ SP (kcal/mol)**	**MM/GBSA DG Bind (kcal/mol)**
CHEMBL938: SARALASIN 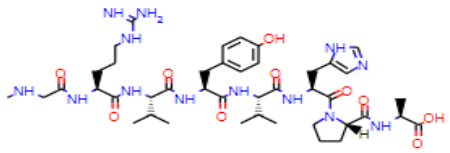	-11.55	-10.23	-119.65
CHEMBL1014: CANDESARTAN CILEXETIL 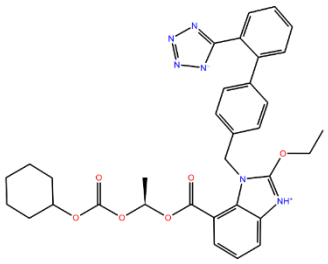	-11.02	-8.76	-116.04
CHEMBL2028661: AZILSARTANMEDOXOMIL	-10.48	-8.56	-107.24

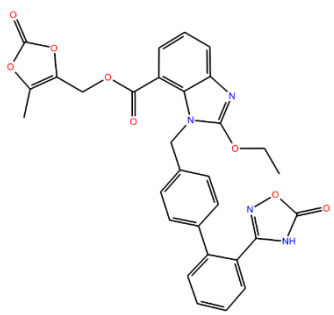			
CHEMBL539423: SPARSENTAN 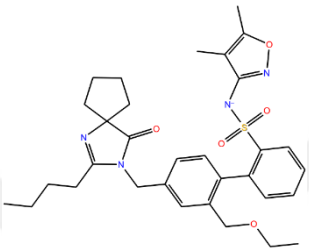	-10.82	-8.49	-87.94
CHEMBL57242: AZILSARTAN 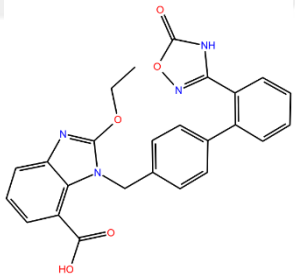	-10.85	-8.13	-81.08
CHEMBL1200692: OLMESARTAN MEDOXOMIL 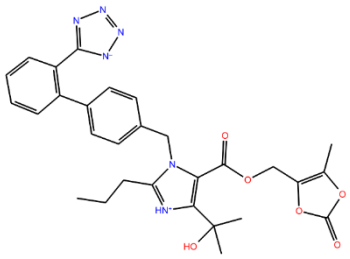	-10.09	-8.86	-96.41

CHEMBL1016: CANDESARTAN 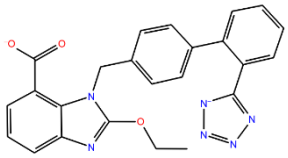	-10.41	-8.22	-92.03
CHEMBL1017: TELMISARTAN 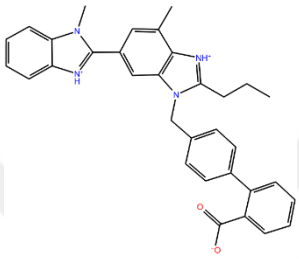	-11.54	-8.39	-113.31

Table 4.4 indicates that saralasin and telmisartan have high docking scores which lines well with the experimental results. Figure 4.4 shows 2D and 3D ligand interactions of telmisartan at the binding pocket of the AT1R.

Figure 4.5: 3D (A) and 2D (B) ligand interaction diagrams of Telmisartan at the binding pocket of AT1R structure.

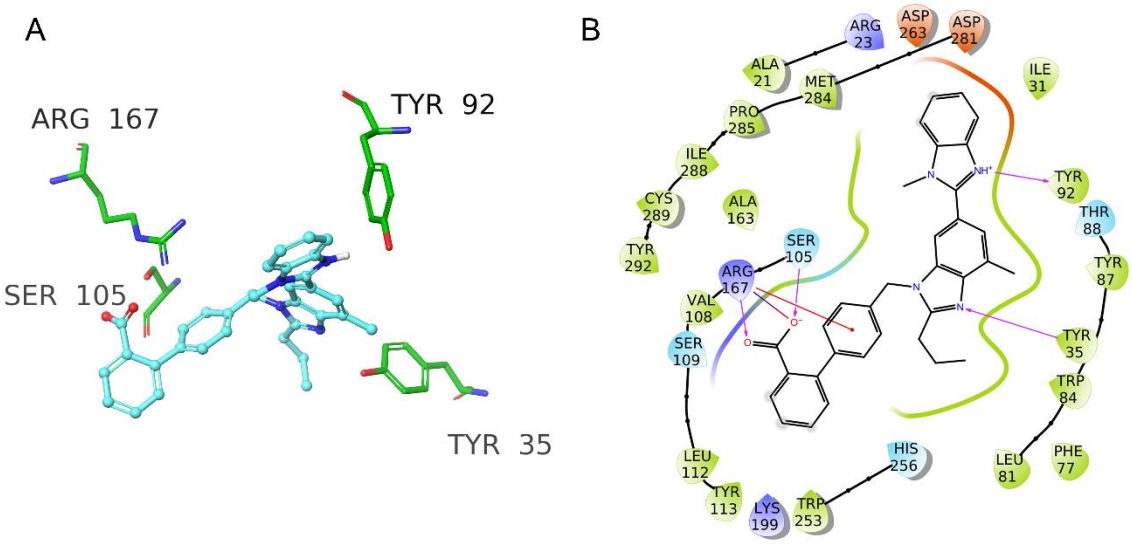

Figure 4.5 indicates that residues Tyr35, Tyr92, and Ser105 construct hydrogen bonding interactions with the ligand. Arg167 forms both hydrogen bonding, pi-cation and salt bridge interactions with the telmisartan.

Table 4.5 represents type of chemical interactions and docking scores of selected known AT1R drugs at the AT1R.

Table 4.5: Top scored selected AT1 drugs and candidates with their docking scores along with their chemical interactions at the active site of AT1R.

Selected AT1 Drugs and Candidates	**Docking Scores (IFD)** **(kcal/mol)**	**Nature Of Interaction**	**Amino Acids on Active Sites**
Saralasin	-11.55	Hydrogen bonding, (backbone), Hydrogen bonding (Side chain), hydrophobic	Lys199, Arg167, Cys180, Asp263, and Asp281
Candesartan Cilexitil	-11.02	Hydrogen bonding, (backbone), Hydrogen bonding (Side chain), hydrophobic	Arg167, Cys180, Asp263, and Asp281
Azilsartan	-10.85	Hydrogen bond ing (backbone), Hydrogen bonding (Side chain), hydrophobic	Arg167, Cys180, Asp263, and Asp281

Table 4.6 shows top-docking scores of selected AT1R binders among docking scores of 2034 compounds.

Table 4.6: Top-scored docking scores of AT1R binders at the binding pocket of AT1R (Docking scores are in kcal/mol).

AT1 BINDERS	2D STRUCTURES	DOCKING SCORE, IFD (kcal/mol)	MM/GBSA BIND kcal/mol
CHEMBL3640124	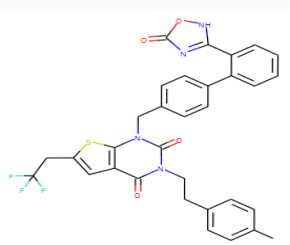	-11.12	-107.39
CHEMBL3640125	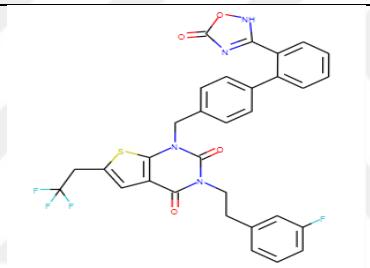	-11.03	-92.51
CHEMBL306638	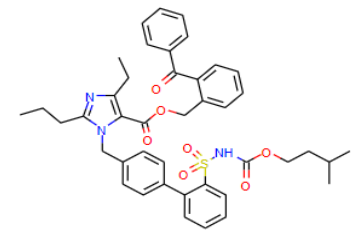	-10.98	-146.80
CHEMBL3640123	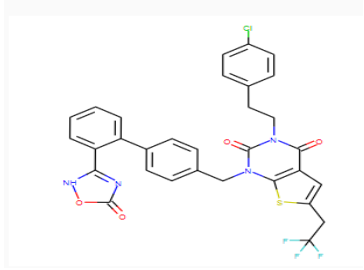	-10.92	-106.88

CHEMBL3640138	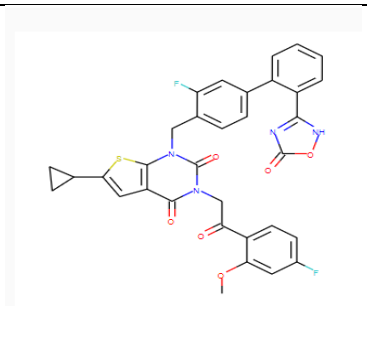	-10.90	-111.67
CHEMBL3640139	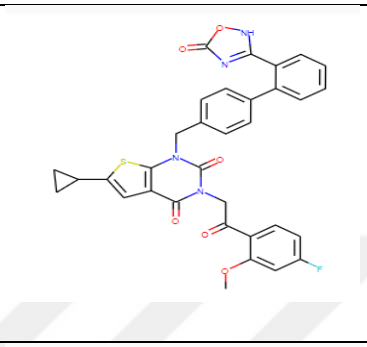	-10.88	-115.22
CHEMBL313868	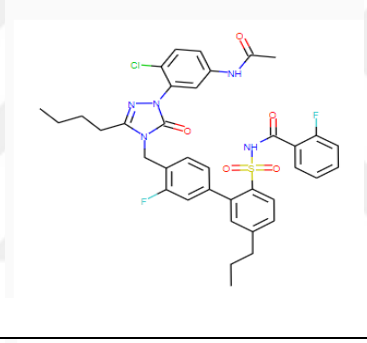	-10.84	-105.37
CHEMBL3735236	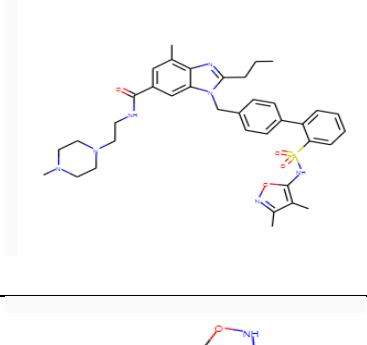	-10.69	-120.60
CHEMBL3640137	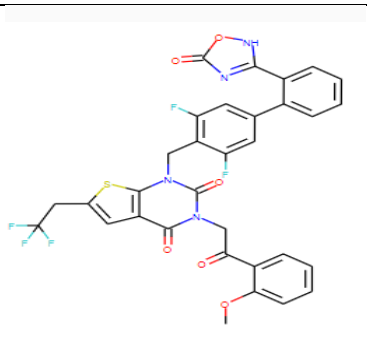	-10.66	-102.30

CHEMBL70100	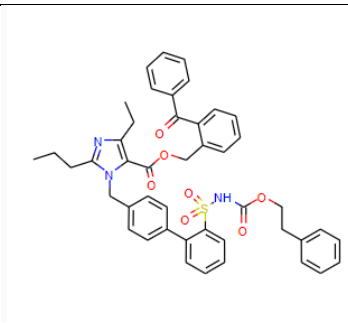	-10.57	-131.10

In order to check the therapeutic activity predictions of selected PARP1 inhibitors at the AT1R, selected hit compounds were also screened at the binary QSAR models of MetaCore/MetaDrug applications of Clarivate Analytics. For this aim, top-20 PARP inhibitors that show predicted high affinity at the AT1R were used. Binary QSAR models of anti-hypertension, anti-inflammation, and anti-cancer models of MetaCore/MetaDrug were used. These models have following statistical results. Hypertension-QSAR model: (Training set: 554, test set: 111, sensitivity: 0.89, specificity: 0.81, accuracy: 0.85; MCC: 0.70); Inflammation-QSAR model: (Training set: 598, test set: 93, sensitivity: 0.86, specificity: 0.84, accuracy: 0.85; MCC: 0.69); Cancer-QSAR model: (Training set: 886, test set: 167, sensitivity: 0.89, specificity: 0.83, accuracy: 0.86; MCC: 0.72). Table 4.7 represent binary QSAR model results of selected PARP inhibitors and their corresponding docking scores at the AT1R.

Table 4.7: Binary QSAR model results of selected top-20 PARP inhibitors.

PARP1 INHIBITORS	2D STRUCTURES	Hypertension QSAR model	Inflammation QSAR model	Cancer QSAR model
CHEMBL 523887	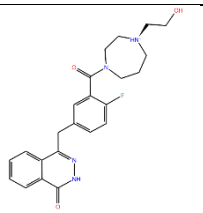	0.41	0.12	0.63
CHEMBL 3945618	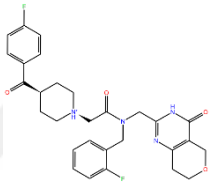	0.59	0.35	0.79
CHEMBL 3317902	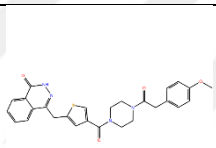	0.52	0.41	0.53
CHEMBL 610491	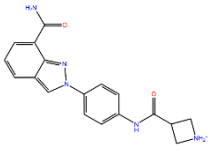	0.56	0.57	0.74
CHEMBL 593609	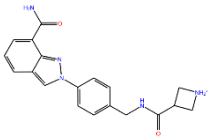	0.50	0.59	0.73
CHEMBL 378794	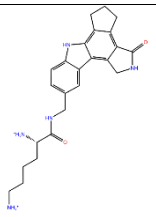	0.59	0.35	0.79

CHEMBL 3933577	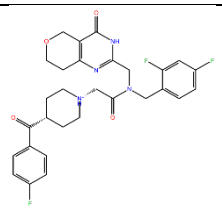	0.91	0.14	0.66
CHEMBL 3105882	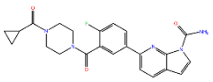	0.41	0.12	0.63
CHEMBL 2323533	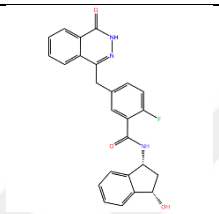	0.32	0.63	0.64
CHEMBL 4177163	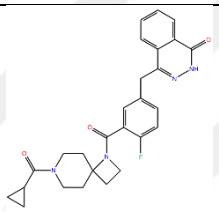	0.55	0.39	0.64
CHEMBL 610165	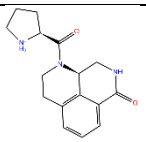	0.57	0.40	0.72
CHEMBL 3663637	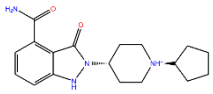	0.62	0.51	0.38
CHEMBL 407760	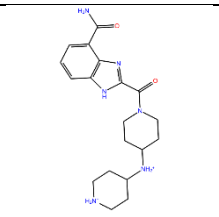	0.63	0.32	0.61

CHEMBL 4084234	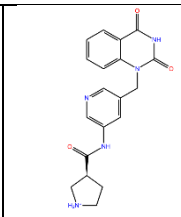	0.39	0.17	0.71
CHEMBL 4167820	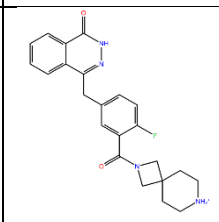	0.62	0.48	0.46
CHEMBL 3649746	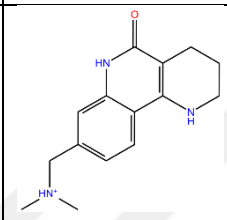	0.52	0.27	0.51
CHEMBL 3922251	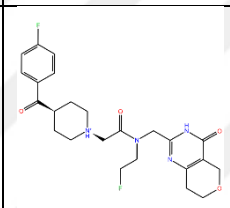	0.91	0.12	0.63
CHEMBL 3891789	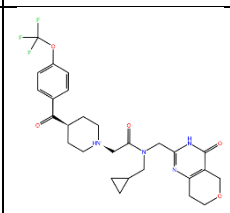	0.91	0.14	0.66
CHEMBL 3644592	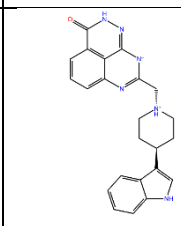	0.71	0.18	0.73

Among the analyzed compounds at three different binary QSAR models, three compounds showed very high predicted therapeutic activity values (0.91) at the hypertension-QSAR models. These molecules were CHEMBL3933577, CHEMBL3922251, and CHEMBL3891789.

Figures 4.6 and 4.7 represent 2D and 3D ligand interaction diagrams of CHEMBL3922251 and CHEMBL3933577 compounds. Corresponding interactions for the CHEMBL3891789 were depicted at Figure 4.2

Figure 4.6: 3D (A) and 2D (B) ligand interactions of CHEMBL3922251 with AT1R (top-docking pose of IFD).

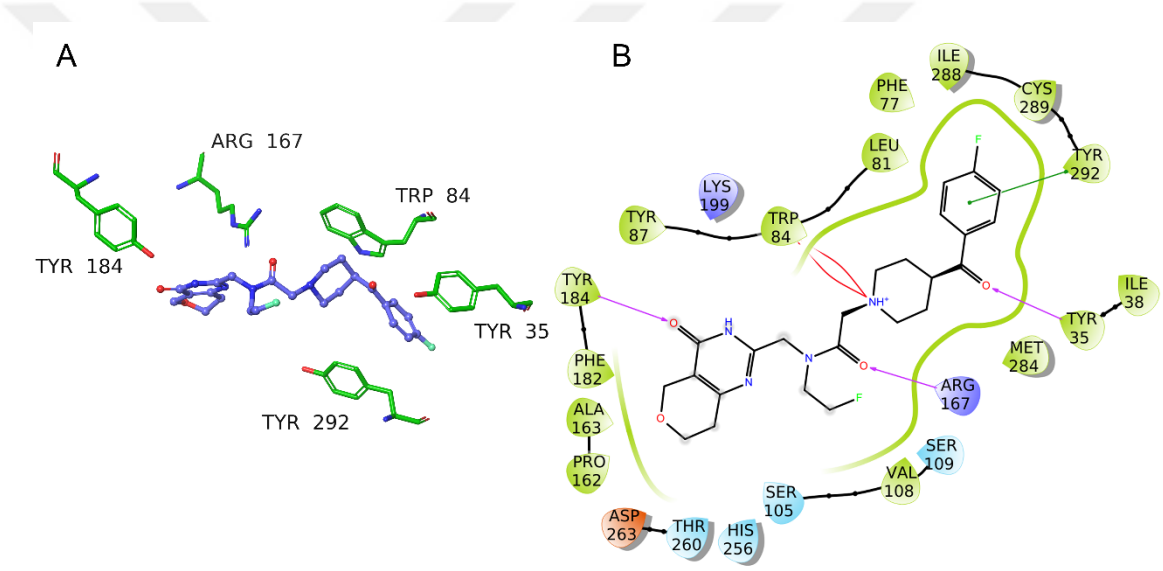

While Tyr35, Arg167, and Tyr184 form hydrogen bonding interactions with the compound (CHEMBL3922251), Trp84 forms pi-cation interactions. Tyr292 constructs pi-pi stacking interactions.

Figure 4.7: 3D (A) and 2D (B) ligand interactions of CHEMBL3933577 with AT1R (top-docking pose of IFD).

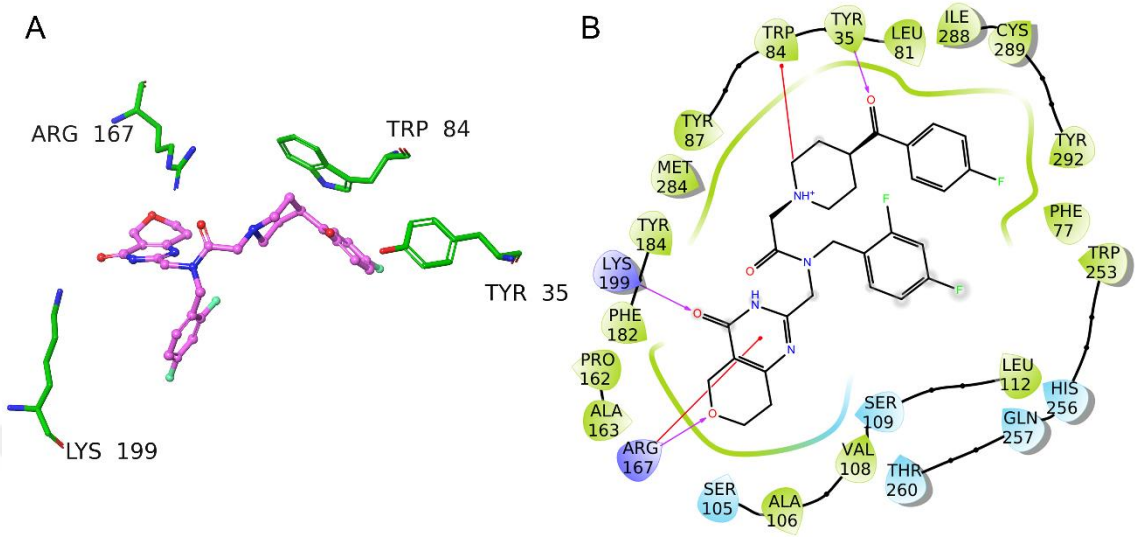

Compound CHEMBL3933577 forms interactions mainly with Tyr35, Trp84, Arg167, and Lys199 which are well-known crucial residues for the ATR blockers.

4.2 MD Simulations

Three selected hit molecules (CHEMBL3933577, CHEMBL3922251, and CHEMBL3891789) were used in MD simulations for better understanding their structural and dynamical profiles at the AT1R. Together with three selected hit compounds, we also used telmisartan as positive control molecule as AT1R antagonist. Figure 4.8 represents change of backbone protein RMSD throughout the simulations when three hit compounds and telmisartan bound to AT1R. All the RMSD values seem in stable form after around 5 ns of MD simulations.

Figure 4.8: RMSD –Time graph comparison of top-3 PARP1 inhibitors used in AT1R for protein backbone, in respect to positive control Telmisartan.

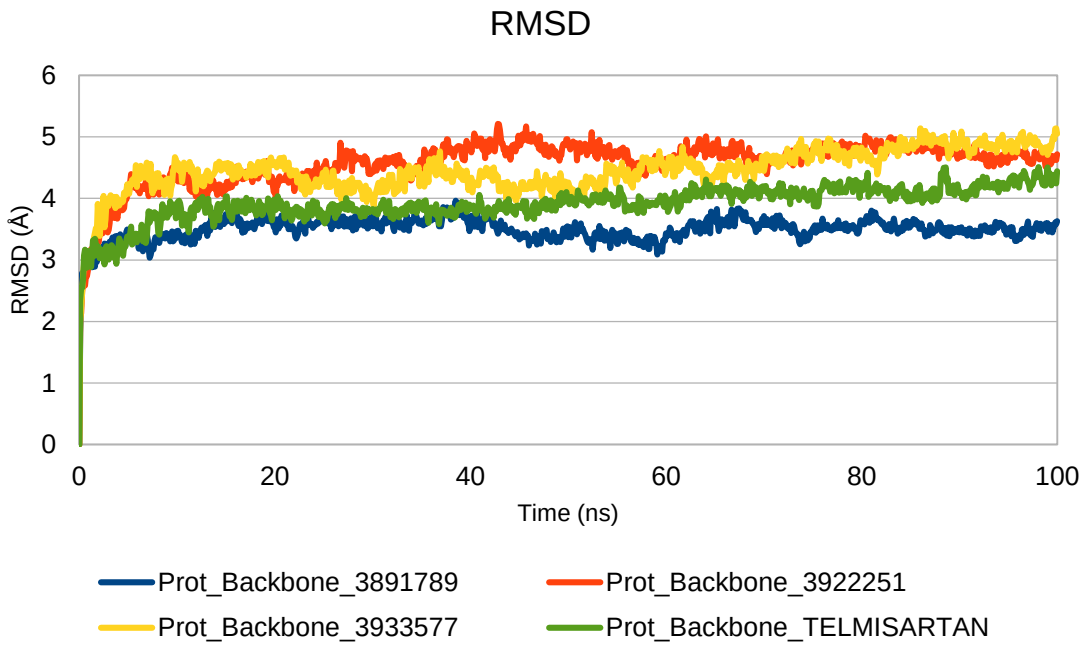

Figure 4.9 depicts representative 2D ligand interactions for CHEMBL3891789. Simulations are repeated 3 times for each system. Here, figure shows representative figure for Run #1.

Figure 4.9: 2D ligand-protein interactions for CHEMBL3891789 during the MD simulations.

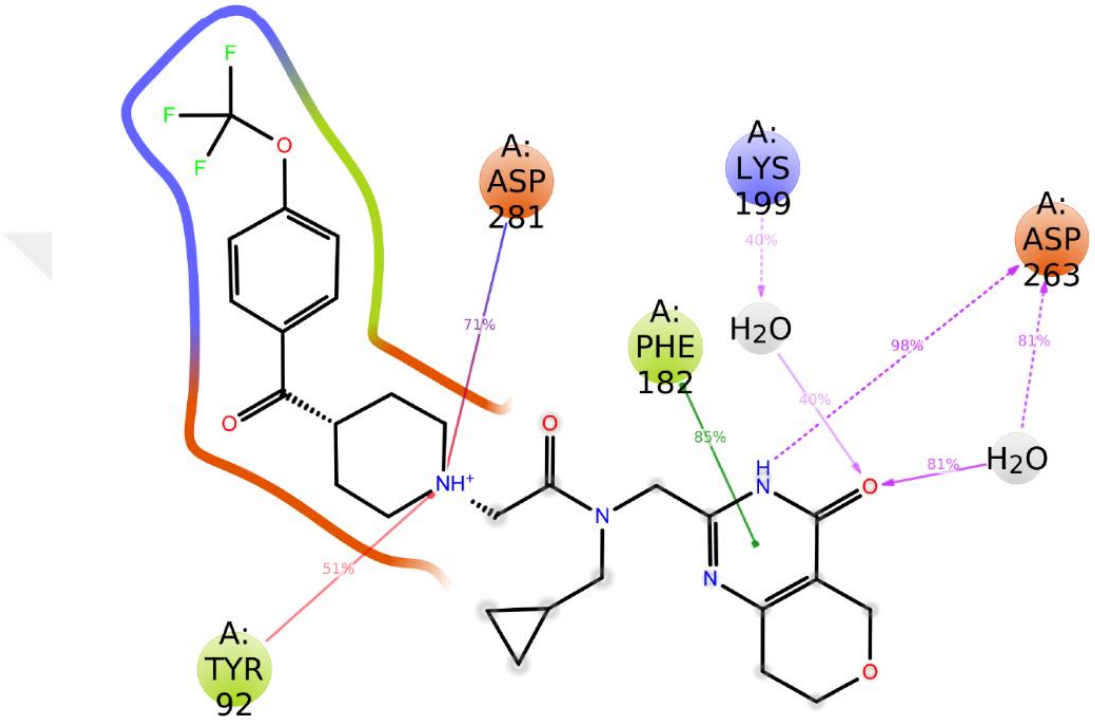

This schematic of detailed ligand atom interactions with protein residues, in which interactions, that occur more than 30% of the simulation time (100 ns) are represented. Protein-ligand interactions can be monitored throughout the simulation. These interactions can be categorized into four types, hydrogen bonds, hydrophobic interactions, ionic interactions and water bridges. H-bonds play a significant role in ligand binding. Hydrogen bonds, between a protein and a ligand can be further broken down into four subtypes: backbone acceptor; backbone donor; side-chain acceptor; side-chain donor. Hydrophobic contacts can be divided into three types, π-Cation; π-π; and other non-specific interactions. Ionic interactions or polar interactions are between two oppositely charged atoms within 3.7 Å and do not involve hydrogen bonds. All ionic interactions can be broken down into two subtypes, mediated by protein backbone or side chains. Water bridges are hydrogen bonded protein-ligand interactions, mediated by

water molecules. The current geometric criteria for protein-water or ligand-water hydrogen bonds are 2.8 Å distance between donor and acceptor atom. Crucial constructed interactions for the binding of CHEMBL3891789 at the AT1R are from Tyr92, Phe182, Lys199, Asp263, and Asp281. While Lys199 and Asp281 mainly forms hydrogen bonds and water bridges, Phe182 constructs pi-pi stacking interactions. Moreover, Asp281 forms ionic interactions and Tyr92 forms pi-cation type interactions. Conservancy of each interactions during the simulations are depicted at the figure.

Figure 4.10 shows 2D ligand-residue interactions of selected hit compound CHEMBL3922251 at the binding pocket of AT1R during the simulations for run#1. While Trp84 and Tyr292 form pi-pi stacking interactions with the ligand, Arg167 and Tyr184 constructs hydrogen bonds.

Figure 4.10: 2D ligand-protein interactions for CHEMBL3922251 during the MD simulations.

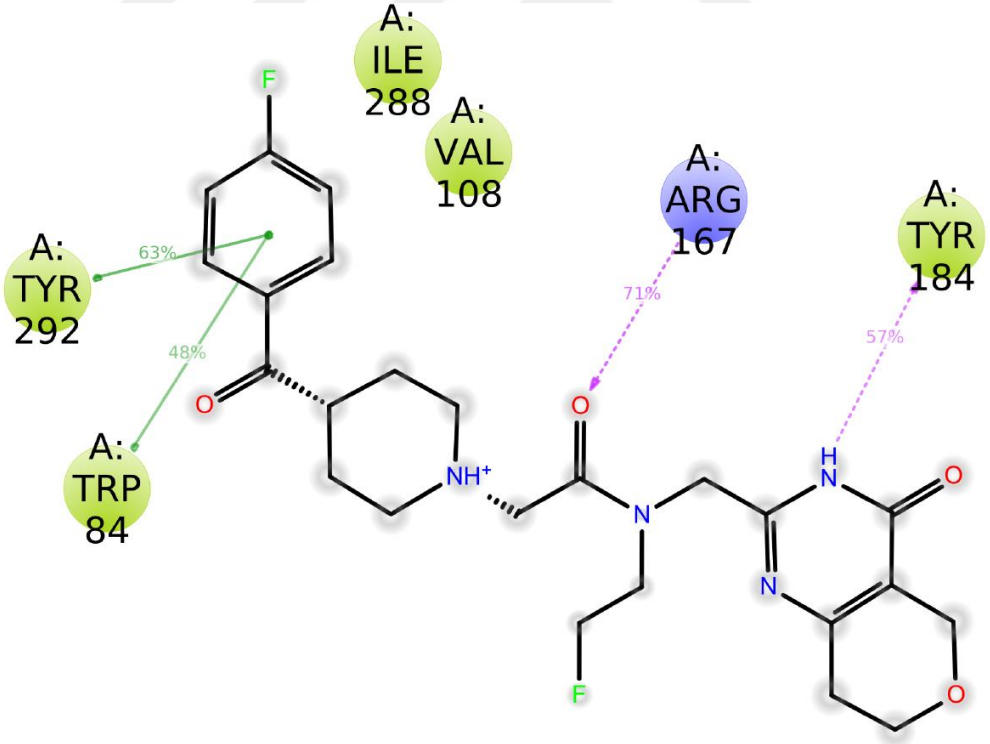

Figure 4.11 represents 2D ligand-residue interactions for CHEMBL3933577 during the simulations. Crucial interactions were from Lys199 (water bridges and hydrogen bonds), Tyr113 (water bridges and hydrogen bonds) and Phe182 and Trp253 (hydrophobic interactions).

Figure 4.11: 2D ligand-protein interactions for CHEMBL3933577 during the MD simulations.

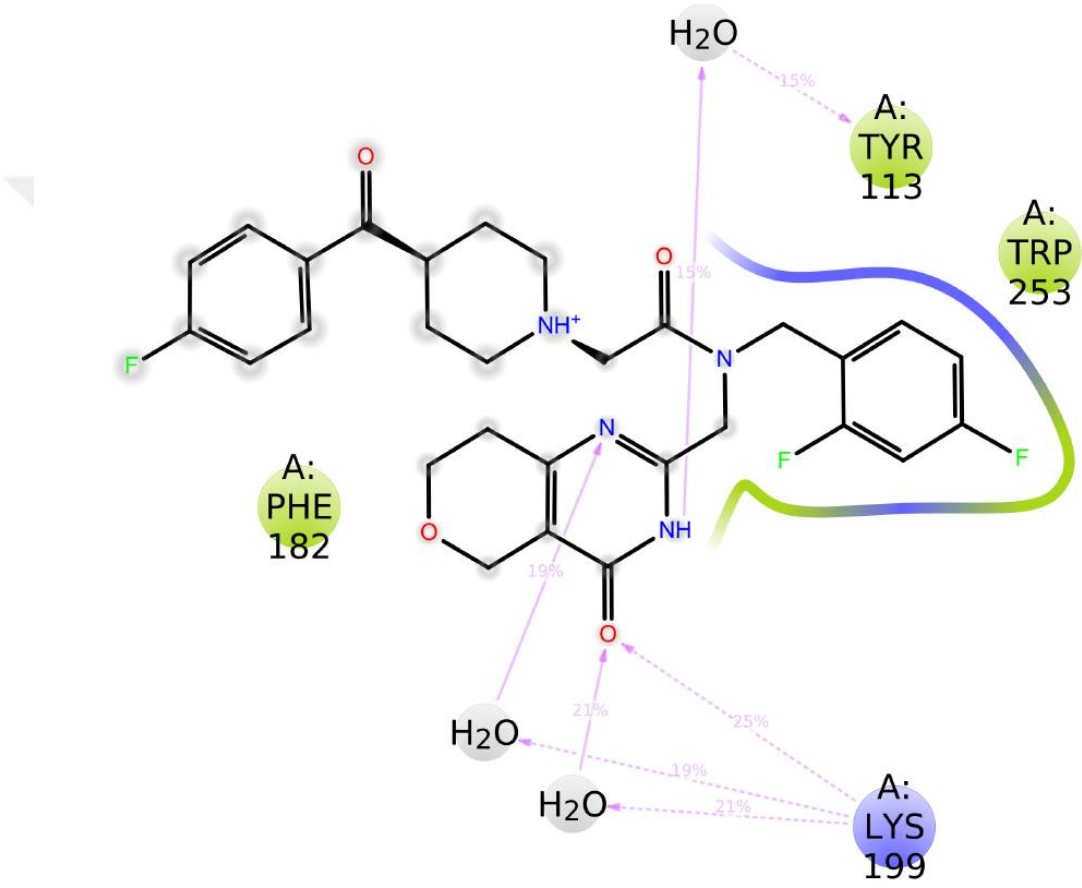

Corresponding protein-ligand interactions during the simulations for positive control compound telmisartan were shown in Figure 4.12. While Arg167, Lys199, Tyr87, Tyr35 form hydrogen bonding interactions, Tyr92 forms pi-pi stacking and pi-cation interactions. Arg167 also forms pi-cation interactions.

Figure 4.12: 2D ligand-protein interactions for Telmisartan during the MD simulations.

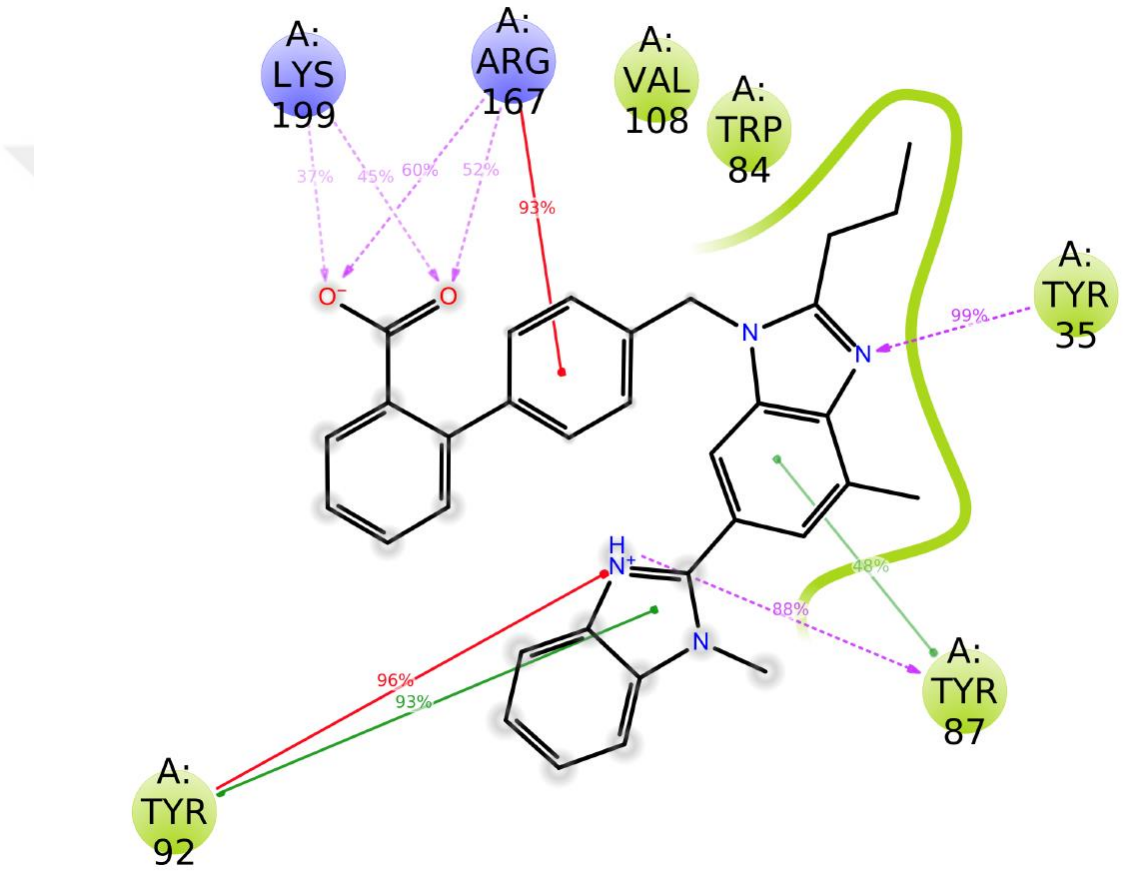

4.3. MM/GBSA Calculations

During the MD simulations, binding free energies of selected three hit compounds and positive control molecule telmisartan were compared. Figure 4.13 shows the change of MM/GBSA during the simulations. It is observed that among three selected compounds CHEMBL3891789 have lower binding free energies than other two selected hits. However, none of the three compounds have found better binding free energies than the positive control telmisartan.

FIGURE 4.13: MM/GBSA –Time graph comparison of top 3 PARP1 inhibitors used in AT1R for MMGBSA ΔG calculation in respect to positive control Telmisartan obtained from 100 ns MD simulations.

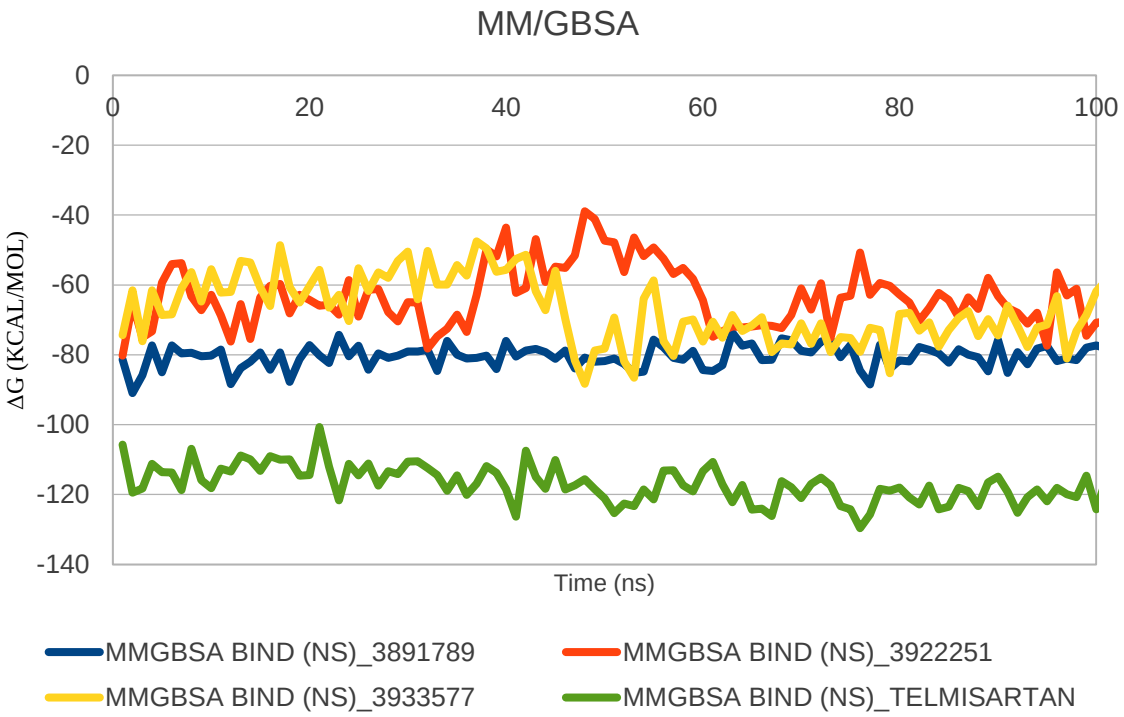

5. DISCUSSION

The purpose of this study was to identify new potential inhibitor against AT1R. Primary focus was searching for a small molecule or ligand that can bind to AT1R and inhibits its activity, so that a potential therapeutic activity can be achieved, which was being desired for intended cure of disease. After analyzing docking scores together with web-based MetaCore/MetaDrug applications, three hit PARP1 inhibitors were chosen, according to their therapeutic activity, which are CHEMBL3891789, CHEMBL3922251 and CHEMBL3977577. These three PARP1 inhibitors showed very competitive docking scores and MM/GBSA scores, compared to marketed drug Telmisartan, which is a very potential AT1R antagonist. Telmisartan has potential cardiovascular effect for treating hypertension and it is considered the most desired drug that inhibits AT1R activity and thus, lowers the blood pressure by putting an affect to blood vessel, responsible for hypertension. Telmisartan has been proven unique among ARB's by its pharmacological along with pharmacokinetic properties (Wienen et al. 2000, Cianchetti et al. 2008, Zı´dek et al. 2013). Telmisartan can bind to AT1R very strongly with a special 'delta lock' structure (Ohno et al. 2011).

Telmisartan was taken as a positive control here, for comparing new inhibitors that can bind to AT1R. The selected top three-scored PARP1 inhibitors showed outstanding predicted antihypertensive value of 0.91 (i.e., all of the three hits have same value of 0.91) with binary hypertension QSAR model and corresponding predicted anticancer values were between 0.61 and 0.63 (Table 4.7). However, selected compounds do not show high predicted antiinflammatory profiles. People with long time diabetes, they do suffer from diabetic retinopathy. Many people for this reason go blind after suffering from long time with diabetes. The top scored three PARP1 inhibitor molecules is being able to bind to AT1R like other AT1R binders and sartan and thus, being able to exert potential effects to a greater extent on the repair mechanism of damages blood vessels. (Yanez et al., 2019)

In order to compare the reliability of docking poses, it is important to consider conformational changes between the ligand of the crystal structure derived from X-ray crystallography and the generated docking poses of ligand by Glide. Docking poses of

ligand generated by Glide, the RMSD values were less than 1.0 Å, which is near to ligand poses of crystal structure. Screening studies, docking studies, MetaCore/MetaDrug applications, and long MD simulations were run to find out potential PARP1 inhibitor that can bind to AT1 receptor for the desired pharmacological effect.

Binding pocket residue-ligand contacts for the selected hit compounds were analyzed in detail and compared with the selected positive control drug telmisartan. Crucial residues for the ligand binding for the telmisartan were found as Arg167, Lys199, Tyr87, Tyr92, and Tyr35 and these contacts were stable (>30%) throughout the simulations. Importance of these residues for high affinity ligand binding were also highlighted in literature. (Ohno et al., 2011; Feng et al., 1995; Yamano et al.,1995; Marie et al. 1994; Groblewski et al. 1997). Among selected hits CHEMBL3922251 represented crucial interactions with following residues: Trp84, Tyr292, Arg167, and Tyr184. Corresponding residues were found as Lys199, Tyr113, Phe182, and Trp253 for CHEMBL3933577 and Tyr92, Phe182, Lys199, Asp263, and Asp281 for CHEMBL3891789.

Although MM/GBSA calculations show very low binding free energies for the selected hits, none of the selected PARP1 inhibitors have lower binding energy values than telmisartan. Among three selected hits, CHEMBL3891789 showed a better predicted binding affinity compared to other two hits at the binding site of the AT1R.

6. CONCLUSIONS

The classic RAS is known as a homeostasis regulator of blood pressure and electrolyte. It has recently been recognized as a pro-inflammatory mediator and implicated in various age-related ocular disorders associated with the activation of inflammatory molecules. The findings of RAS components in the eye initiate a new therapeutic approach to alleviate ocular disorders through RAS inhibitors such as AT1R antagonists. It is shown that retinal microglia express AT1R and their activation state is significantly altered by its endogenous ligand Ang-II. Thus, Ang-II may directly activate the AT1Rs on microglia and contribute to retinal inflammation, such as in diabetic retinopathy, an increase in Ang-II levels play an important role. Since it is shown that microglia-mediated inflammation response in the retina has been associated with the development of retinal degenerations and because of therapeutic effects of PARP1 inhibitors on retinal degeneration, in this study, known PARP1 inhibitors have collected from CHEMBL database and screened at the binding pocket residues of the AT1R.

In this study, several molecular screening methods and computational approaches of molecular docking and MD simulations were performed and at the end, we selected three PARP1 inhibitors as hit compounds which are CHEMBL3891789, CHEMBL3933577, and CHEMBL3922251. Both structural and energetic results of the selected hits were compared with the known AT1R inhibitor telmisartan. At the study, both rigid and flexible docking approaches as well as molecular dynamics simulations were performed. Moreover, binary QSAR models were used to predict the potential therapeutic activities of the selected hit compounds. We propose that these three selected hit compounds (PARP1 inhibitors) may have important therapeutic profiles retinal inflammation. However, in order to validate the *in silico* results in this study, *in vitro* tests must be carried out.

7. REFERENCES

PERIODICALS

A, T., & VA, B., 2018. Molecular Docking: From Lock and Key to Combination Lock. *Journal of Molecular Medicine and Clinical Applications*, **2** (1), pp. 1–19. doi: 10.16966/2575-0305.106

Amé, J. C., Spenlehauer, C., & De Murcia, G., 2004. The PARP superfamily. *BioEssays*, **26** (8), pp. 882–893. doi.org/ 10.1002/bies.20085

Anderson, S. D., Tabassum, A., Yeon, J. K., Sharma, G., Santos, P., Soong, T. Thu, Y. W., Nies, I., Kurita, T., Chandler, A., Alsamarah, A., Kanassatega, R. S., Luo, Y. L., Botello-Smith, W. M., & Andresen, B. T., 2020. In silico prediction of ARB resistance: A first step in creating personalized ARB therapy. *PLoS Computational Biology*, **16** (11), pp. 1–23. doi: 10.1371/journal.pcbi.1007719

Bei, Y., 2017. *Physiology & Behavior*, **176** (3), pp. 139–148. doi: 10.1016/j.addr.2016.

Bolcato, G., Bissaro, M., Sturlese, M., & Moro, S., 2020. Comparing fragment binding poses prediction using HSP90 as a key study: When bound water makes the difference. *Molecules*, **25** (20), p. 4651. https://doi.org/10.3390/molecules25204651

Breiding, M. J., 2014. HHS Public Access. *Physiology & Behavior*, **63** (8), pp. 1–18.

Berman, H. M., Battistuz, T., Bhat, T. N., Bluhm, W. F., Bourne, P. E., Burkhardt, K., Feng, Z., Gilliland, G. L., Iype, L., Jain, S., Fagan, P., Marvin, J., Padilla, D., Ravichandran, V., Schneider, B., Thanki, N., Weissig, H., Westbrook, J. D. & Zardecki, C., 2002. The Protein Data Bank. *Acta Crystallogr D Biol Crystallogr*, **58**, pp. 899-907. https:// doi.org/ 10.1107/s0907444902003451

Bas, D. C., Rogers, D. M. & Jensen, J. H., 2008. Very Fast Prediction and Rationalization Of Pka Values For Protein–Ligand Complexes. *Proteins:*

Structure, Function, And Bioinformatics, **73** (3), pp. 765-783. https:// doi.org/ 10.1002/prot.22102

Chen, A., 2011. PARP inhibitors: its role in treatment of cancer. *Chinese Journal of Cancer*, **30** (7), pp. 463–471. https:// doi.org/10.5732/cjc.011.10111

Coppo, M., Bandinelli, M., Chiostri, M., Poggesi, L., & Boddi, M., 2017. Persistent and selective upregulation of renin–Angiotensin system in circulating T lymphocytes in unstable Angina. *JRAAS - Journal of the Renin-Angiotensin-Aldosterone System*, **18** (1), pp. 1–8. https:// doi.org/10.1177/1470320317698849

Cherezov, V., Rosenbaum, D. M., Hanson, M. A., Rasmussen, S. G. F., Thian, F. S., Kobilka, T. S., Choi, H.-J., Kuhn, P., Weis, W. I., Kobilka, B. K. & Stevens, R. C., 2007. High Resolution Crystal Structure Of An Engineered Human B (2) Adrenergic G Protein-Coupled Receptor. *Science (New York, N.Y.)*, **318** (5854), pp. 1258-1265. https:// doi.org/10.1126/science.1150577

Davies, M. N., Toseland, C. P., Moss, D. S., & Flower, D. R., 2006. Benchmarking pKa prediction. *BMC Biochemistry*, **7** (18), pp. 1–12. https:// doi.org/ 10.1186/1471-2091-7-18.

De Gasparo, M., Catt, K., Inagami, T., Wright, J. & Unger, T., 2000. International Union of Pharmacology. Xxiii. The Angiotensin Ii Receptors. *Pharmacological Reviews*, **52**, pp. 415-472.

Eustermann, S., Wu, W. F., LAngelier, M. F., Yang, J. C., Easton, L. E., Riccio, A. A., Pascal, J. M., & Neuhaus, D., 2015. Structural Basis of Detection and Signaling of DNA Single-Strand Breaks by Human PARP-1. *Molecular Cell*, **60** (5), pp. 742–754. https:// doi.org/10.1016/j.molcel.2015.10.032

Ferreira, L. G., Dos Santos, R. N., Oliva, G., & Andricopulo, A. D., 2015. Molecular docking and structure-based drug design strategies. In *Molecules*, **20** (7), pp. 13384-421. https:// doi.org/10.3390/molecules200713384

Fredriksson, R., Lagerstrom, M. C., Lundin, L. G. & Schioth, H. B., 2003a. The G-ProteinCoupled Receptors In The Human Genome Form Five Main Families. Phylogenetic Analysis, Paralogon Groups, And Fingerprints. *Mol Pharmacol*, **63** (6), pp. 1256-72. https:// doi.org/ 10.1124/mol.63.6.1256.

Fredriksson, R., Lagerström, M. C., Lundin, L.-G. & Schiöth, H. B., 2003b. The GProtein-Coupled Receptors In The Human Genome Form Five Main Families. Phylogenetic Analysis, Paralogon Groups, And Fingerprints. *Molecular Pharmacology*, **63**, p. 1256. https://doi.org/10.1124/mol.63.6.1256

Friesner, R. A., Banks, J. L., Murphy, R. B., Halgren, T. A., Klicic, J. J., Mainz, D. T., Repasky, M. P., Knoll, E. H., Shelley, M. & Perry, J. K., 2004a. Glide: A New Approach For Rapid, Accurate Docking And Scoring. 1. Method And Assessment of Docking Accuracy. *Journal of Medicinal Chemistry*, **47**, pp. 1739-1749

Friesner, R. A., Banks, J. L., Murphy, R. B., Halgren, T. A., Klicic, J. J., Mainz, D. T., Repasky, M. P., Knoll, E. H., Shelley, M., Perry, J. K., Shaw, D. E., Francis, P. & Shenkin, P. S., 2004b. Glide: A New Approach For Rapid, Accurate Docking And Scoring. 1. Method And Assessment Of Docking Accuracy. *J Med Chem*, **47**, pp. 1739-49.

Friesner, R. A., Murphy, R. B., Repasky, M. P., Frye, L. L., Greenwood, J. R., Halgren, T. A., Sanschagrin, P. C. & Mainz, D. T., 2006. Extra Precision Glide: Docking And Scoring Incorporating A Model Of Hydrophobic Enclosure For Protein Ligand Complexes. *Journal Of Medicinal Chemistry*, **49**, pp. 6177-6196. https:// doi.org/10.1021/jm051256o

Gradman, A. H., 2002. AT1-receptor blockers: differences that matter. *Journal of Human Hypertension*, *16(3)*, pp. S9–S16. https:// doi.org/ 10.1038/sj.jhh.1001434

Gurevich, V. V., & Gurevich, E. V., 2019. GPCR signaling regulation: The role of GRKs and arrestins. *Frontiers in Pharmacology*, **10** (2), pp. 1–11. https:// doi.org/10.3389/fphar.2019.00125

Greenwood, J. R., Calkins, D., Sullivan, A. P. & Shelley, J. C., 2010. Towards The Comprehensive, Rapid, And Accurate Prediction Of The Favorable Tautomeric States Of Drug-Like Molecules In Aqueous Solution. *Journal Of Computer-Aided Molecular Design*, **24** (6), pp. 591-604. https:// doi.org/ 10.1007/s10822-010-9349-1.

Halgren, T. A., Murphy, R. B., Friesner, R. A., Beard, H. S., Frye, L. L., Pollard, W. T. & Banks, J. L., 2004. Glide: A New Approach For Rapid, Accurate Docking And

Scoring. 2. Enrichment Factors In Database Screening. *Journal Of Medicinal Chemistry*, **47** (7), pp. 1750-1759. https:// doi.org/ 10.1021/jm030644s

Huambachano, O., Herrera, F., Rancourt, A., & Satoh, M. S., 2011. Double-stranded DNA binding domain of poly (ADP-ribose) polymerase-1 and molecular insight into the regulation of its activity. *Journal of Biological Chemistry*, **286** (9), pp. 7149–7160. https:// doi.org/10.1074/jbc.M110.175190

Ivanova, L., Tammiku-Taul, J., García-Sosa, A. T., Sidorova, Y., Saarma, M., & Karelson, M., 2018. Molecular Dynamics Simulations of the Interactions between Glial Cell Line-Derived Neurotrophic Factor Family Receptor GFRα1 and Small-Molecule Ligands. *ACS Omega*, **3** (9), pp. 11407–11414. https:// doi.org/ 10.1021/acsomega.8b01524

Jean-Charles, P. Y., Kaur, S., & Shenoy, S. K., 2017. G Protein-Coupled Receptor Signaling Through β-Arrestin-Dependent Mechanisms. In *Journal of Cardiovascular Pharmacology*, **70** (3), pp. 142-158. https:// doi.org/ 10.1097/FJC.0000000000000482

Kawai, T., Forrester, S. J., O'Brien, S., Baggett, A., Rizzo, V., & Eguchi, S., 2017. AT1 receptor signaling pathways in the cardiovascular system. *Pharmacological Research*, **125**, pp. 4–13. https:// doi.org/ 10.1016/j.phrs.2017.05.008

Ko, H. L., & Ren, E. C., 2012. Functional aspects of PARP1 in DNA repair and transcription. *Biomolecules*, **2** (4), pp. 524–548. https://doi.org/10.3390/biom2040524

Kunert-Radek, J., Stepień, H., Komorowski, J., & Pawlikowski, M., 1994. Stimulatory effect of Angiotensin II on the proliferation of mouse spleen lymphocytes in vitro is mediated via both types of Angiotensin II receptors. In *Biochemical and Biophysical Research Communications*, **198** (3), pp. 1034–1039. https:// doi.org/10.1006/bbrc.1994.1147

Kitchen, D. B., Decornez, H., Furr, J. R. & Bajorath, J., 2004. Docking And Scoring In Virtual Screening For Drug Discovery: Methods And Applications. *Nat Rev Drug Discov*, **3**, pp. 935-49. https://doi.org/10.1038/nrd1549

Kruse, A. C., Hu, J., Pan, A. C., Arlow, D. H., Rosenbaum, D. M., Rosemond, E., Green, H. F., Liu, T., Chae, P. S., Dror, R. O., Shaw, D. E., Weis, W. I., Wess, J. & Kobilka, B., 2012. Structure and Dynamics Of The M (3) Muscarinic Acetylcholine Receptor. *Nature*, **482**, pp. 552-556. https:// doi.org/10.1038/nature10867

Kurihara, T., Ozawa, Y., Ishida, S., Okano, H., & Tsubota, K., 2012. Renin-Angiotensin system hyperactivation can induce inflammation and retinal neural dysfunction. *International Journal of Inflammation*, **2012**, pp. 1-14. https:// doi.org/ 10.1155/2012/581695

Li, H., Robertson, A. D. & Jensen, J. H., 2005. Very Fast Empirical Prediction And Rationalization Of Protein Pka Values. *Proteins: Structure, Function, And Bioinformatics*, **61** (4), pp. 704-721. https:// doi.org/ 10.1002/prot.20660

Lionta, E., Spyrou, G., Vassilatis, D., & Cournia, Z., 2014. Structure-Based Virtual Screening for Drug Discovery: Principles, Applications and Recent Advances. *Current Topics in Medicinal Chemistry*, **14** (16), pp. 1923–1938. https:// doi.org/10.2174/1568026614666140929124445

Lorenz-Fonfria, V. A., 2020. Infrared Difference Spectroscopy of Proteins: From Bands to Bonds. *Chemical Reviews*, **120** (7), pp. 3466–3576. https://doi.org/10.1021/acs.chemrev.9b00449

Malyuchenko, N. V., Kotova, E. Y., Kulaeva, O. I., Kirpichnikov, M. P., & Studitskiy, V. M., 2015. PARP1 Inhibitors: Antitumor drug design(1) Malyuchenko, N. V., Kotova, E. Y., Kulaeva, O. I., Kirpichnikov, M. P., and Studitskiy, V. M., 2015. PARP1 Inhibitors: Antitumor drug design. Acta Naturae. *Acta Naturae*, **7** (3), pp. 27–37.

Miura, S. I., Karnik, S. S., & Saku, K., 2011. Angiotensin II type 1 receptor blockers: Class effects versus molecular effects. *JRAAS - Journal of the Renin-Angiotensin-Aldosterone System*, **12** (1), pp. 1–7. https:// doi.org/ 10.1177/1470320310370852

Murata, M. M., Kong, X., Moncada, E., Chen, Y., Imamura, H., WAng, P., Berns, M. W., Yokomori, K., & Digman, M. A., 2019. NAD+ consumption by PARP1 in response to DNA damage triggers metabolic shift critical for damaged cell

survival. *Molecular Biology of the Cell*, **30** (20), pp. 2584–2597. https:// doi.org/10.1091/mbc.E18-10-0650

Nguyen, C., Yamazaki, T., Kovalenko, A., Case, D. A., Gilson, M. K., Kurtzman, T., & Luchko, T., 2019. A molecular reconstruction approach to site-based 3D-RISM and comparison to GIST hydration thermodynamic maps in an enzyme active site. *PLoS ONE*, **14** (7), pp. 1–19. https://doi.org/10.1371/journal.pone.0219473

Patel, M., Nowsheen, S., Maraboyina, S., & Xia, F., 2020. The role of poly (ADP-ribose) polymerase inhibitors in the treatment of cancer and methods to overcome resistance: A review. *Cell and Bioscience*, **10** (1), pp. 1–12. https://doi.org/10.1186/s13578-020-00390-7

Paul, S. M., Mytelka, D. S., Dunwiddie, C. T., Persinger, C. C., Munos, B. H., Lindborg, S. R. & Schacht, A. L., 2010. How To Improve R&D Productivity: The Pharmaceutical Industry's Grand Challenge. *Nat Rev Drug Discov*, **9** (3), pp. 203-14. https:// doi.org/ 10.1038/nrd3078

Preston, R. A., Materson, B. J., Reda, D. J. & Et Al., 1998. Age-Race Subgroup Compared with Renin Profile As Predictors Of Blood Pressure Response to Antihypertensive Therapy. *Jama*, **280** (13), pp. 1168-1172. https:// doi.org/10.1001/jama.280.13.1168

Rastelli, G., Del Rio, A., Degliesposti, G. & Sgobba, M., 2010. Fast And Accurate Predictions Of Binding Free Energies Using Mm-Pbsa And Mm-Gbsa. *J Comput Chem*, **31** (4), pp. 797-810. https:// doi.org/ 10.1002/jcc.21372

Reinemund, J., Seidel, K., Steckelings, U. M., Zaade, D., Klare, S., Rompe, F., Katerbaum, M., Schacherl, J., Li, Y., Menk, M., Schefe, J. H., Goldin-Lang, P., Szabo, C., Olah, G., Unger, T., & Funke-Kaiser, H., 2009. Poly (ADP-ribose) polymerase-1 (PARP-1) transcriptionally regulates angiotensin AT2 receptor (AT2R) and AT2R binding protein (ATBP) genes. *Biochemical Pharmacology*, **77** (12), pp. 1795–1805. https:// doi.org/ 10.1016/j.bcp.2009.02.025

Roos, K., Wu, C., Damm, W., Reboul, M., Stevenson, J. M., Lu, C., Dahlgren, M. K., Mondal, S., Chen, W., WAng, L., Abel, R., Friesner, R. A., & Harder, E. D., 2019. OPLS3e: Extending Force Field Coverage for Drug-Like Small Molecules

[Research-article]. *Journal of Chemical Theory and Computation*, **15** (3), pp. 1863–1874. https://doi.org/ 10.1021/acs.jctc.8b01026

Rübsam, A., Parikh, S., & Fort, P. E., 2018. Role of inflammation in diabetic retinopathy. *International Journal of Molecular Sciences*, **19** (4), pp. 1–31. https://doi.org/10.3390/ijms19040942

Sallander, J., Wallinder, C., Hallberg, A., Aqvist, J. & Gutierrez-De-Teran, H., 2016. Structural Determinants Of Subtype Selectivity And Functional Activity Of Angiotensin Ii Receptors. *Bioorg Med Chem Lett*, **26**, pp. 1355-9. https:// doi.org/ 10.1016/j.bmcl.2015.10.084

Salo-ahen, O. M. H., Alanko, I., Bhadane, R., Bonvin, A. M. J. J., Honorato, R. V., Hossain, S., Juffer, A. H., Kabedev, A., Lahtela-kakkonen, M., Larsen, A. S., Lescrinier, E., & Marimuthu, P., 2021. *Pharmaceutical Development*. pp. 1–60.

Sastry, G. M., Adzhigirey, M., Day, T., Annabhimoju, R. & Sherman, W., 2013. Protein And Ligand Preparation: Parameters, Protocols, And Influence On Virtual Screening Enrichments. *Journal Of Computer-Aided Molecular Design*, **27**, pp. 221-34.

Scott A. Hollingsworth, & Ron O. Dror, 2018. Molecular dynamics simulation for all. *Neuron*, **99**, pp. 1129–1143. https:// doi.org/ 10.1016/j.neuron.2018.08.011

Shelley, J. C., Cholleti, A., Frye, L. L., Greenwood, J. R., Timlin, M. R. & Uchimaya, M., 2007. Epik: A Software Program For Pk A Prediction And Protonation State Generation For Drug-Like Molecules. *Journal Of Computer-Aided Molecular Design*, **21**, pp. 681-691. https://doi.org/ 10.1007/s10822-007-9133-z

Silva-Filho, J. L., Caruso-Neves, C., & Pinheiro, A. A. S., 2016. Angiotensin II type-1 receptor (AT1 R) regulates expansion, differentiation, and functional capacity of antigen-specific CD8+ T cells. *Scientific Reports*, **6**, pp. 1–17. https://doi.org/10.1038/srep35997

Singh, K. D., & Muthusamy, K., 2013. Molecular modeling, quantum polarized ligand docking and structure-based 3D-QSAR analysis of the imidazole series as dual KT1 and ET A receptor antagonists. *Acta Pharmacologica Sinica*, **34** (12), pp. 1592–1606. https:// doi.org/10.1038/aps.2013.129

Sjølie, A. K., & Chaturvedi, N., 2002. The retinal renin-Angiotensin system: Implications for therapy in diabetic retinopathy. *Journal of Human Hypertension*, **16**, pp. S42–S46. https://doi.org/10.1038/sj.jhh.1001438

Sliwoski, G., Kothiwale, S., Meiler, J., & Lowe, E. W., 2014. Computational methods in drug discovery. *Pharmacological Reviews*, **66** (1), pp. 334–395. https://doi.org/10.1124/pr.112.007336

Sun, D., Shen, W., Zhang, F., Fan, H., Tan, J., Li, L., Xu, C., Zhang, H., Yang, Y., & Cheng, H., 2018. α -Hederin Arrests Cell Cycle at G2/M Checkpoint and Promotes Mitochondrial Apoptosis by Blocking Nuclear Factor- B Signaling in Colon Cancer Cells. *BioMed Research International*, *2018*.

Talevi, A., 2018. Computer-aided drug design: An overview. *Methods in Molecular Biology*, **1762** (5), pp. 1–19. https:// doi: 10.1007/978-1-4939-7756-7_1

Ulbig, M. W., & Kollias, A. N., 2010. Diabetische Retinopathie: Frühzeitige Diagnostik und Effiziente Therapie. *Deutsches Arzteblatt*, **107** (5), pp. 75–84.

Van Gastel, J., Hendrickx, J. O., Leysen, H., Santos-Otte, P., Luttrell, L. M., Martin, B., & Maudsley, S., 2018. β-Arrestin based receptor signaling paradigms: Potential therapeutic targets for complex age-related disorders. *Frontiers in Pharmacology*, **9** (11), pp. 1–21. https://doi.org/10.3389/fphar.2018.01369

Verma, J., Khedkar, V. M. & Coutinho, E. C., 2010. 3D-QSAR In Drug Design- A Review. *Curr Top Med Chem*, **10**, pp. 95-115. https:// doi: 10.2174/156802610790232260

Wang, D., 2018. The essential role of G protein-coupled receptor (GPCR) signaling in regulating T cell immunity. *Immunopharmacology and Immunotoxicology*, **40** (3), pp. 187–192. https:// doi: 10.1080/08923973.2018.1434792

Wang, Y. Q., Wang, P. Y., Wang, Y. T., Yang, G. F., Zhang, A., & Miao, Z. H., 2016. An update on poly (ADP-ribose) polymerase-1 (PARP-1) inhibitors: Opportunities and challenges in cancer therapy. *Journal of Medicinal Chemistry*, **59** (21), pp. 9575–9598. https:// doi: 10.1021/acs.jmedchem.6b00055

Wang, Z., Sun, H., Yao, X., Li, D., Xu, L., Li, Y., Tian, S., & Hou, T., 2016. Comprehensive evaluation of ten docking programs on a diverse set of protein-

ligand complexes: The prediction accuracy of sampling power and scoring power. *Physical Chemistry Chemical Physics*, **18** (18), pp. 12964–12975.

Yanez, M., Jhanji, M., Murphy, K., Gower, R. M., Sajish, M., & Jabbarzadeh, E., 2019. Nicotinamide Augments the Anti-Inflammatory Properties of Resveratrol through PARP1 Activation. *Scientific Reports*, **9** (1), pp. 1–10. https://doi.org/10.1038/s41598-019-46678-8

Yang, J., Shen, C., & Huang, N., 2020. Predicting or Pretending: Artificial Intelligence for Protein-Ligand Interactions Lack of Sufficiently Large and Unbiased Datasets. *Frontiers in Pharmacology*, **11** (2), pp. 1–9. https:// doi.org/ 10.3389/fphar.2020.00069

Yu, W., & Mackerell, A. D., 2017. Docking and scoring in virtual screening for drug discovery. *Methods in Molecular Biology*, **1520**, pp. 85–106. https:// doi: 10.1007/978-1-4939-6634-9_5

Zhang, H., Unal, H., Desnoyer, R., Han, G. W., Patel, N., Katritch, V., Karnik, S. S., Cherezov, V. & Stevens, R. C., 2015a. Structural Basis For Ligand Recognition And Functional Selectivity At Angiotensin Receptor. *Journal Of Biological Chemistry,* **290**, pp. 29127-29139. https:// doi: 10.1074/jbc.M115.689000

Zhang, Z., Chang, X., Zhang, C., Zeng, S., Liang, M., Ma, Z., Wang, Z., Huang, W., & Shen, Z., 2020. Identification of probe-quality degraders for Poly (ADP-ribose) polymerase-1 (PARP-1). *Journal of Enzyme Inhibition and Medicinal Chemistry*, **35** (1), pp. 1606–1615. https:// doi:10.1080/14756366.2020.1804382

Zhou, Q., Yang, D., Wu, M., Guo, Y., Guo, W., Zhong, L., Cai, X., Dai, A., Jang, W., Shakhnovich, E., Liu, Z. J., Stevens, R. C., Lambert, N. A., Babu, M. M., WAng, M. W., & Zhao, S., 2019. *Common activation mechanism of class a GPCRs*. *ELife*, **8**, pp. 1–31. https:// doi: 10.7554/eLife.50279